Novel Metal-to-Metal Silyl-Migration Reactions in Heterometallic Complexes

Pierre Braunstein,*[a] Michael Knorr,[a, d] Georg Reinhard,[b] Ulrich Schubert,[b, c] and Thomas Stährfeldt[a]

Dedicated to Professor J. Amaudrut, on the occasion of his 60th birthday

Abstract: An unprecedented, intramolecular metal-to-metal silyl ligand migration reaction has been discovered in a series of phosphido-bridged iron-platinum complexes and which may be triggered by an external nucleophile. Thus, reaction of solutions of $[(OC)_3(R^1_3Si)Fe(\mu\text{-}PR^2R^3)Pt(1,5\text{-}COD)]$ (**1a** $R^1 = OMe$, $R^2 = R^3 = Ph$; **1b** $R^1 = OMe$, $R^2 = R^3 = Cy$; **1c** $R^1 = Ph$, $R^2 = R^3 = Ph$; **1d** $R^1 = Ph$, $R^2 = R^3 = Cy$; **1e** $R^1 = Ph$, $R^2 = H$, $R^3 = Ph$) in CH_2Cl_2 with CO rapidly afforded the corresponding complexes $[(OC)_4Fe(\mu\text{-}PR^2R^3)Pt(SiR^1_3)(CO)]$ (**2a**–**e**) in which the silyl ligand has migrated from Fe to Pt, while two CO ligands have been ligated, one on each metal. When **1a** or **1c** was slowly treated with two equivalents of *t*BuNC at low temperature, quantitative displacement of the COD ligand was accompagnied by silyl migration from Fe to Pt and coordination of an isonitrile ligand to Fe and to Pt to give $[(OC)_3(tBuNC)Fe(\mu\text{-}PPh_2)Pt\{Si(OMe)_3\}(CNtBu)]$ (**3a**) and $[(OC)_3(tBuNC)Fe(\mu\text{-}PPh_2)Pt\{SiPh_3\}(CNtBu)]$ (**3c**). Reaction of **2a** with one equivalent of *t*BuNC selectively led to substitution of the Pt-bound CO to give $[(OC)_4Fe(\mu\text{-}PCy_2)Pt\{Si(OMe)_3\}(CNtBu)]$ (**4b**), which reacted with a second equivalent of *t*BuNC to give $[(OC)_4Fe(\mu\text{-}PCy_2)Pt\{Si(OMe)_3\}(CNtBu)_2]$ (**5b**) in which the metal–metal bond has been cleaved. Opening of the Fe–Pt bond was also observed upon reaction of **3a** with *t*BuNC to give $[(OC)_3(tBuNC)Fe(\mu\text{-}PPh_2)Pt\{Si(OMe)_3\}(CNtBu)_2]$ (**6**). The silyl ligand migrates from Fe, in which it is *trans* to μ-PR^2R^3 in all the metal–metal-bonded complexes, to a position *cis* to the phosphido bridge on Pt. However, in **5a**,**b** and **6** with no metal–metal bond, the Pt-bound silyl ligand is *trans* to the phosphido bridge. The intramolecular nature of the silyl migration, which may be formally viewed as a redox reaction, was established by a cross-over experiment consisting of the reaction of **1a** and **1d** with CO; this yielded exclusively **2a** and **2d**. The course of the silyl-migration reaction was found to depend a) on the steric properties of the $-SiR^1_3$ ligand, and for a given μ-PR^2R^3 bridge ($R^2 = R^3 = Ph$), the migration rate decreases in the sequence $Si(OMe)_3 > SiMe_2Ph > SiMePh_2 \gg SiPh_3$; b) on the phosphido bridge and for a given silyl ligand ($R^1 = OMe$), the migration rate decreases in the order μ-$PPh_2 \gg \mu$-PHCy; c) on the external nucleophile since reaction of **1c** with two equivalents of $P(OMe)_3$, $P(OPh)_3$ or $Ph_2PCH_2C(O)Ph$ led solely to displacement of the COD ligand with formation of **11a**–**c**, respectively, whereas reaction with two equivalents of *t*BuNC gave the product of silyl migration **3c**. Reaction of $[(OC)_3\{(MeO)_3Si\}Fe(\mu\text{-}PPh_2)Pt(PPh_3)_2]$ (**7a**) with *t*BuNC (even in slight excess) occurred stereoselectively with replacement of the PPh_3 ligand *trans* to μ-PPh_2, whereas reaction with CO led first to $[(OC)_3\{(MeO)_3Si\}Fe(\mu\text{-}PPh_2)Pt(CO)(PPh_3)]$ (**8a**), which then isomerized to the migration product $[(OC)_4Fe(\mu\text{-}PPh_2)Pt\{Si(OMe)_3\}(PPh_3)]$ (**9a**). Most complexes were characterized by elemental analysis, IR and ^1H, ^{31}P, ^{13}C, and ^{29}Si NMR spectroscopy, and in five cases by X-ray diffraction.

Keywords: bimetallic complexes · iron · P ligands · platinum · Si ligands · silyl migration

[a] Dr. P. Braunstein, Dr. M. Knorr, T. Stährfeldt
Laboratoire de Chimie de Coordination (UMR 7513 CNRS)
Institut Le Bel, Université Louis Pasteur
4 rue Blaise Pascal, 67070 Strasbourg (France)
Fax: (+33) 3-88-41-60-30
E-mail: braunst@chimie.u-strasbg.fr

[b] G. Reinhard, Prof. Dr. U. Schubert
Institut für Anorganische Chemie der Universität Würzburg
Am Hubland, 97074 Würzburg (Germany)

[c] Prof. Dr. U. Schubert
Institut für Anorganische Chemie
der Technischen Universität Wien
Getreidemarkt 9, 1060 Wien (Austria)

[d] Dr. M. Knorr
New address: Laboratoire de Chimie et Electrochimie Moléculaire
Faculté des Sciences et Techniques
Université de Franche-Comté
16 Route de Gray, 25030 Besançon (France)
E-mail: michael.knorr@univ-fcomte.fr

Introduction

The increasing interest in organosilicon chemistry has been triggered by recent synthetic and mechanistic discoveries of fundamental importance and by advanced applications.[1–3] A rich and versatile chemistry is not unexpected for an element like silicon, which can be surrounded in its compounds by a number of neighbors ranging from one (e.g., Si≡O) to ten (e.g., $Si(C_5Me_5)_2$). Synthetic and reactivity studies on metal–silicon bonds have become a major research area in organometallic chemistry and although the first transition metal silyl complex $[Cp(OC)_2Fe\text{-}SiMe_3]$ was reported more than 40 years ago,[4] the nature of the metal–silicon bond is still the subject of thermodynamic, spectroscopic, and theoretical studies.[1–3] In this context, it is interesting that *heterobimetallic* silicon chemistry has only recently become a well-identified research

  0947-6539/00/0623-4265 $ 17.50+.50/0

topic where novel and unexpected features can arise.[5] In focusing our interest on alkoxysilyl $-Si(OR)_3$ and siloxysilyl $-Si(OSiR_3)_3$ derivatives, we have, for example, discovered that these ligands are able to bridge between two adjacent metal centers by forming a η^2-μ_2-Si-O interaction in a four-membered ring structure (Scheme 1).

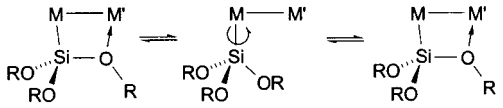

Scheme 1. Formation and dynamic behavior of a η^2-μ_2-Si-O interaction.

An unprecedented lability of the dative $SiO \rightarrow M'$ bond has been observed in stable Fe–Pd complexes such as $[(OC)_3Fe\{\mu\text{-}Si(OMe)_2(OMe)(\mu\text{-}dppm)Pd]$ (X = Cl, Me; dppm = bis(diphenylphosphino)methane), and we could take advantage of the resulting masked coordination site available on palladium to perform multi-insertion of organic isonitriles, sequential CO/olefin insertion into the Pd-Me bond,[6, 7] or catalytic dehydrogenative coupling of stannanes.[8, 9] In the course of our studies on the carbonylation of alkyl complexes, we observed a bimetallic rearrangement involving migration of the iron-bound alkoxysilyl or siloxysilyl ligand to the oxygen atom of the palladium-bound acyl ligand, thus leading to a rare example of bridging siloxycarbene ligand [Eq. (1)].[10]

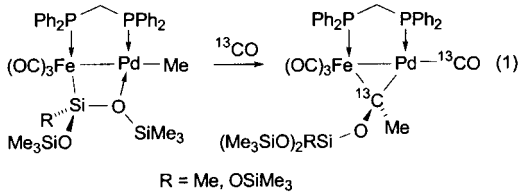

R = Me, $OSiMe_3$

Whereas silyl-migration reactions can lead to the formation of Si–C, Si–P or Si–O bonds,[1a,b,2] the first example of 1,2-silyl group migration from one metal to another was described by our group only recently.[11]

Here we report investigations on a series of phosphido-bridged heterometallic Fe–Pt complexes of the type $[(OC)_3(R^1_3Si)Fe(\mu\text{-}PR^2R^3)PtL^1L^2]$ that enabled us to identify the factors leading to migration reactions of a silyl ligand from iron to platinum. This required a general synthetic access to this class of compounds in order to allow variations of R^1, R^2, R^3 and L and study their respective influence on this reaction. It will be shown that it is important to introduce a labile ligand on platinum, such as COD (COD = 1,5-cyclooctadiene), that can be subsequently easily displaced. The replacement of a Fe–Si bond by a Pt–Si bond under mild conditions is particularly notable, since platinum is known to be a key element in catalysts for numerous reactions in silicon chemistry.[12]

Results and Discussion

Heterodinuclear complexes of the type $[(OC)_3(R^1_3Si)Fe(\mu\text{-}PR^2R^3)Pt(1,5\text{-}COD)]$ (**1**) were prepared in good yields (75–90%) by reaction of a CH_2Cl_2 or toluene solution of $[HFe(SiR^1_3)(CO)_3(PHR^2R^3)]$ with a stoichiometric amount of $[Pt(1,5\text{-}COD)_2]$ at 0 °C (Scheme 2).

Two different reaction sequences leading to **1a–e** are conceivable, since oxidative addition across Pt^0 could occur first with the P–H and then the Fe–H bond (Scheme 2a) or

Abstract in French: *Une nouvelle réaction chimique, la migration intramoléculaire d'un ligand silyle d'un métal vers un autre, a été observée et étudiée dans une famille de complexes hétérobimétalliques Fe – Pt à pont phosphure. Cette réaction peut être déclanchée par des réactifs nucléophiles. Ainsi, la réaction de $[(OC)_3(R^1_3Si)Fe(\mu\text{-}PR^2R^3)Pt(1,5\text{-}COD)]$ (**1a** $R^1 = OMe$, $R^2 = R^3 = Ph$; **1b** $R^1 = OMe$, $R^2 = R^3 = Cy$; **1c** $R^1 = Ph$, $R^2 = R^3 = Ph$; **1d** $R^1 = Ph$, $R^2 = R^3 = Cy$; **1e** $R^1 = Ph$, $R^2 = H$, $R^3 = Ph$) dans CH_2Cl_2 avec CO conduit rapidement aux complexes correspondants $[(OC)_4Fe(\mu\text{-}PR^2R^3)Pt(SiR^1_3)(CO)]$ (**2a–e**) dans lesquels le ligand silyle a migré du Fe au Pt alors que deux ligands CO ont été coordinés, un sur chaque métal. La réaction de **1a** ou **1c** avec 2 équiv de tBuNC à basse température conduit quantitativement au déplacement du ligand COD et à la migration du groupement silyle du Fe vers le Pt pour $[(OC)_3(tBuNC)Fe(\mu\text{-}PPh_2)Pt\{Si(OMe)_3\}(CNtBu)]$ (**3a**) et $[(OC)_3(tBuNC)Fe(\mu\text{-}PPh_2)Pt\{SiPh_3\}(CNtBu)]$ (**3c**). La réaction de **2a** avec 1 équiv de tBuNC conduit sélectivement à la substitution du CO lié au Pt pour donner $[(OC)_4Fe(\mu\text{-}PCy_2)Pt\{Si(OMe)_3\}(CNtBu)]$ (**4b**), lequel réagit avec un deuxième équiv de tBuNC pour former $[(OC)_4Fe(\mu\text{-}PCy_2)Pt\{Si(OMe)_3\}(CNtBu)_2]$ (**5b**) dans lequel la liaison métal-métal a été ouverte. La réaction of **3a** avec tBuNC conduit également à l'ouverture de la liaison Fe – Pt pour donner $[(OC)_3(tBuNC)Fe(\mu\text{-}PPh_2)Pt\{Si(OMe)_3\}(CNtBu)_2]$ (**6**). Dans le cas des complexes à liaison métal-métal, le ligand silyle migre du fer, où il se trouve en trans du pont $\mu\text{-}PR^2R^3$ vers le platine, en position cis de ce pont. Par contre, dans le cas de **5a,b** et **6** qui ne contiennent pas de liaison métal-métal, the ligand silyle se retrouve sur le platine en position trans du pont phosphuro. Cette réaction de migration de silyle, qui peut formellement être décrite comme une réaction rédox intramoléculaire, dépend a) des propriétés stériques du ligand $-SiR^1_3$ et, pour un pont $\mu\text{-}PR^2R^3$ donné ($R^2 = R^3 = Ph$), la vitesse de migration décroit dans l'ordre $Si(OMe)_3 > SiMe_2Ph > SiMePh_2 \gg SiPh_3$; b) de la nature des substituants sur le pont phosphuro et, pour un ligand silyle donné ($R^1 = OMe$), la vitesse de migration décroit dans l'ordre $PPh_2 \gg PHCy$; (c) du nucléophile externe puisque la réaction de **1c** avec 2 equiv $P(OMe)_3$, $P(OPh)_3$ ou $Ph_2PCH_2C(O)Ph$ n'a conduit qu'au déplacement du ligand COD et formation de **11a–c**, alors que la réaction avec 2 equiv de tBuNC conduit, après migration de silyle, à **3c**. La réaction de $[(OC)_3\{(MeO)_3Si\}Fe(\mu\text{-}PPh_2)Pt(PPh_3)_2]$ (**7a**) avec tBuNC (même en léger excès) se déroule de manière stéréosélective par remplacement du ligand PPh_3 situé en trans de $\mu\text{-}PPh_2$ alors que la réaction avec CO conduit d'abord à $[(OC)_3\{(MeO)_3Si\}Fe(\mu\text{-}PPh_2)Pt(CO)(PPh_3)]$ (**8a**) qui s'isomérise ensuite en $[(OC)_4Fe(\mu\text{-}PPh_2)Pt\{Si(OMe)_3\}(PPh_3)]$ (**9a**). En général, les complexes ont été caractérisés par analyse élémentaire et spectroscopies IR et RMN (^1H, ^{31}P, ^{13}C et ^{29}Si) et par diffraction des rayons X pour 5 d'entre eux.*

0947-6539/00/0623-4266 $ 17.50+.50/0 *Chem. Eur. J.* **2000**, *6*, No. 23

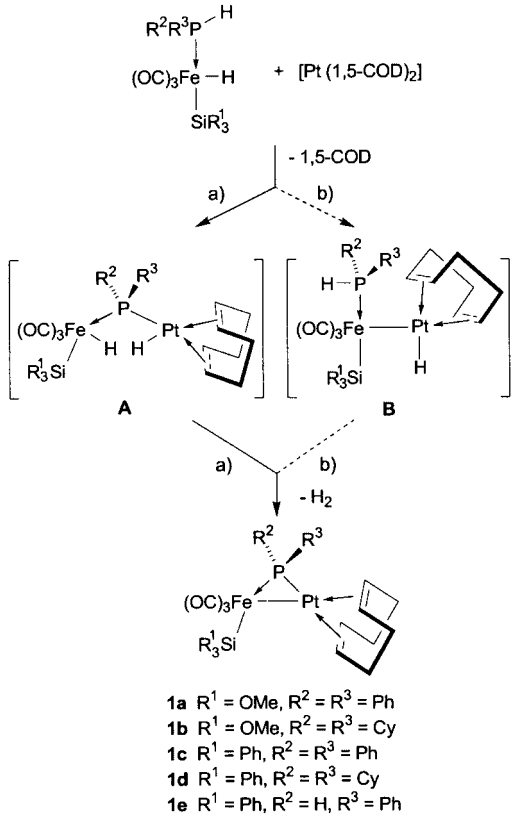

Scheme 2. Possible pathways to the formation of complexes **1a–e** (see text).

vice-versa (Scheme 2b). We believe that oxidative addition of the P–H bond to Pt^0 occurs first, resulting in a phosphido-bridged intermediate **A** and is followed by reductive elimination of H_2 to give the product. It is known from other investigations that the P–H bond of coordinated secondary phosphines is very reactive, notably in the case of PPh_2H, leading readily to phosphido-bridged complexes.[13–16] Silane elimination was not observed although this is a conceivable reaction which has been observed in bimetallic Fe–Rh[17] and Fe–Re complexes.[18] By analogy with the dinuclear oxidative addition of molecular hydrogen across a metal–metal bond, and in order to obey the microreversibility principle, reductive elimination of hydrogen from a dinuclear complex of the type $[L_n(H)M\text{-}(\mu\text{-}PR_2)\text{-}M'(H)L'_m]$ can, in principle, occur sequentially by hydrogen migration followed by reductive elimination of H_2 from one metal center or by simultaneous elimination from the two metal centers.[19] The role of the electronic configuration of the metals has been analyzed theoretically, but we are not aware of studies concerning reductive elimination of H_2 from a d^6–d^8 system resulting in metal-metal bond formation or, conversely, oxidative addition of H_2 to d^7–d^9 centers. The low symmetry of intermediate **A** in Scheme 2 and its flexibility due to the absence of metal–metal bonding could account for the observation that release of H_2 is evidently faster than insertion of the 1,5-COD ligand into the Pt–H bond, a step previously observed in the synthesis of a Fe–Pt cyclooctenyl complex of the π-allylic type.[20] Reaction intermediates could not be observed by ^1H NMR spectroscopy owing to very fast reactions: the product is formed already after a few seconds at $-60\,^\circ C$ in toluene.

Since a C=C double bond of the COD ligand in **1** is *trans* to Fe and the other *trans* to the μ-P atom, the ^1H NMR spectrum shows two singlets with ^{195}Pt satellites for the olefinic protons, as observed, for example, in $[PtCl(CF{=}CF_2)(1,5\text{-}COD)]$.[21] When the steric bulk of the silyl ligand increases, the singlet corresponding to the protons of the C=C double bond *trans* to μ-P, which are closer to the silyl substituents, shifts to higher field, whereas the other singlet remains unaffected. The $^{31}P\{^1H\}$ NMR chemical shift of the phosphido ligand is strongly dependent on the phosphorus substituents, and this resonance is shifted downfield by about 60 ppm on going from $\mu\text{-}PPh_2$ to $\mu\text{-}PCy_2$ for both $R^1 = OMe$ and Ph. The $^1J(Pt,P)$ coupling constant is approximately 3000 Hz in **1a–d** and 3206 Hz in **1e**.[22] The three ν(CO) absorptions observed for **1a–e** in solution are consistent with the meridional arrangement of the CO ligands found in the solid state.[20] The coordination geometry about the Fe center may be viewed as distorted octahedral or better, trigonal bipyramidal when the metal–metal bond is neglected. A comparison between complexes **1d** and **1e** shows that the stronger electron-donating ability of the $\mu\text{-}PCy_2$ bridge is felt by the iron center and this causes a shift of the ν(CO) bands toward lower wavenumbers.

The reaction of solutions of complexes **1a–e** in CH_2Cl_2 with CO rapidly afforded the complexes $[(OC)_4Fe(\mu\text{-}PR^2R^3)Pt(SiR^1_3)(CO)]$ (**2a–e**) as orange oily substances which are soluble in pentane and difficult to crystallize [Eq. (2)]. When the CO atmosphere was replaced with nitrogen or when the solvent was removed under reduced pressure, these complexes slowly decomposed and only two derivatives, **2b** and **2c**, could be isolated pure, and both were characterized by X-ray diffraction (see below).

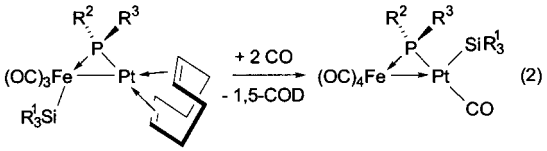

1a R^1 = OMe, $R^2 = R^3$ = Ph
1b R^1 = OMe, $R^2 = R^3$ = Cy
1c R^1 = Ph, $R^2 = R^3$ = Ph
1d R^1 = Ph, $R^2 = R^3$ = Cy
1e R^1 = Ph, R^2 = H, R^3 = Ph

2a R^1 = OMe, $R^2 = R^3$ = Ph
2b R^1 = OMe, $R^2 = R^3$ = Cy
2c R^1 = Ph, $R^2 = R^3$ = Ph
2d R^1 = Ph, $R^2 = R^3$ = Cy
2e R^1 = Ph, R^2 = H, R^3 = Ph

The migration of the silyl ligand from Fe to Pt was unambiguously established by $^{29}Si\{^1H\}$ NMR spectroscopy. The doublet observed for **1a** at $\delta = 7.3$ ($^2J(P,Si) = 23$ Hz, $^2J(Pt,Si) = 49$ Hz) is shifted to -26.8 ($^2J(P,Si) = 4$ Hz) in **2a** with a strong $^1J(Pt,Si)$ coupling of 2117 Hz. The small value of 4 Hz for $^2J(P,Si)$ is indicative of a *cis* arrangement of the μ-P and Si nuclei in **2a**. For comparison, a $^2J(P,Si)$ coupling of 33.5 Hz was observed in $[(OC)_3\{(MeO)_3Si\}Fe(\mu\text{-}dppm)Pd(\eta^3\text{-}MeC_3H_4)]$ in which the P-Fe-Si angle is almost 180°.[23] The ^1H, $^{13}C\{^1H\}$, and $^{29}Si\{^1H\}$ NMR data are given in the Experimental Section and selected $^{31}P\{^1H\}$ NMR and IR ν(CO) spectroscopic data are presented in Table 1.

The ν(CO) vibration for the Pt-bound carbonyl in **2a–e** occurs around 2075 cm^{-1} and those for the Fe-bound CO

Table 1. Selected $^{31}P\{^1H\}$ NMR [δ in ppm and J in Hz] and IR data [cm^{-1}] for the μ-phosphido complexes.

	δ (μ-PR_2)	δ (PPh_3)	^2J(P,P)	^1J(Pt,μ-P)	^1J(Pt,P)	ν(CN) and ν(CO)[a]
1a	140.9[b]			3007		1983 (s), 1918 (s), 1901 (s)
1b	199.6[b]			2961		1973 (s), 1905 (s), 1887 (s)
1c	152.9[b]			3054		1973 (s), 1912 (s), 1892 (s)
1d	209.7[b]			2994		1964 (s), 1901 (s), 1882 (s)
1e	113.2[b]			3206		1995 (s), 1939 (s), 1921 (s)
2a	125.1[c]			2597		2079 (s), 2047 (s), 2004 (s,sh), 1992 (vs), 1968 (w,sh)
2b	150.4[c]			2261		2072 (s), 2040 (s), 1986 (s), 1970 (s), 1949 (s,sh)
2c	128.0[c]			2755		2077 (s), 2047 (s), 2006 (s,sh), 1992 (s), 1974 (w,sh)
2d	153.1[c]			2390		2069 (vs), 2039 (vs), 1986 (s), 1965 (m), 1950 (m,sh)
2e	79.3[c]			2521		2079 (vs), 2049 (vs), 2008 (s,sh), 2000 (vs), 1982 (m,sh)
3a	140.5[c]			2687		2168 (s), 2143 (w,sh), 2009 (vs), 1956 (s), 1943 (s)
3c	139.8[c]			2829		2166 (s), 2149 (w,sh), 2002 (vs), 1945 (s), 1936 (s)
4b	141.9[c]			2314		2179 (s), 2036 (vs), 1968 (s), 1942 (s)
5a	49.2[c]			1063		2199 (s), 2027 (s), 1945 (s), 1914 (vs)
5b	61.7[c]			1133		2188 (s), 2018 (s), 1934 (s), 1904 (vs)
6	62.3[c]			1056		2194 (vs), 2135 (s), 1959 (w), 1885 (s), 1872 (s)
8a	159.5[b]	28.4	13	2657	3422	2061 (m), 1989 (m), 1928 (s,br)
8b	163.6[b]	26.9	16	2589	3436	2055 (m), 1974 (m), 1910 (sh), 1902 (vs)
8c	167.6[b]	27.7	15	2579	3439	2058 (m), 1975 (m), 1910 (sh), 1902 (vs)
8d	171.3[b]	26.2	13	2625	3456	2060 (m), 1973 (m), 1915 (sh), 1902 (vs)
8e	146.7[c]	27.6		2290	3110	2047 (s), 2005 (vs), 1952 (s), 1938 (s)
9a	116.9[b]	36.0	308	2125	3027	2040 (vs), 1975 (m), 1949 (s), 1927 (s)
9b	118.5[b]	31.4	315	2324	3168	2034 (vs), 1972 (s), 1945 (s), 1920 (s)
9c	121.7[c]	31.2	314	2304	3136	2037 (vs), 1974 (s), 1947 (s), 1920 (s)
10	70.6[c]	36.4	283	1829	3073	2042 (vs), 2004 (w), 1975 (s), 1952 (s), 1929 (s)
12a	153.0[b]	24.4	7	2709	3618	2180 (s), 1969 (s), 1900 (br vs)
12b	135.1[b]	28.3	<3	2507	3541	2170 (m), 1995 (vs), 1935 (s), 1920 (s)
12c	156.9[b]	25.9	7	2695	3588	2177 (m), 1962 (s), 1897 (br vs)
12d	136.5[b]	27.6	5	2443	3515	2139 (m), 1997 (vs), 1937 (s), 1922 (s)
12e	154.8[b]	26.6	9	2622	3555	2140 (m), 1957 (m), 1890 (sh), 1875 (s)
12f	161.7[d]	26.3	9	2677	3570	2150 (s), 1966 (s), 1903 (vs), 1886 (vs)

[a] In CH_2Cl_2. [b] In C_6D_6. [c] In $CDCl_3$. [d] In CD_2Cl_2.

ligands are significantly shifted toward higher wavenumbers relative to those in **1a–e**, as the result of a decreased electron density at iron. This is due to the replacement of the silyl ligand by a π-acceptor CO ligand and of the COD ligand at Pt by a silyl and a CO ligand.

The remarkable silyl-migration reaction leading to **2a–e** was too fast to allow any intermediate to be observed, such as $[(OC)_3(R^1_3Si)\overline{Fe(\mu\text{-}PR^2R^3)}Pt(CO)_2]$ which would simply result from substitution of COD by two CO ligands. The crystal structures of **2b** and **2c** were determined by X-ray diffraction (Figures 1 and 2). Selected bond lengths and angles are given in Tables 2 and 3.

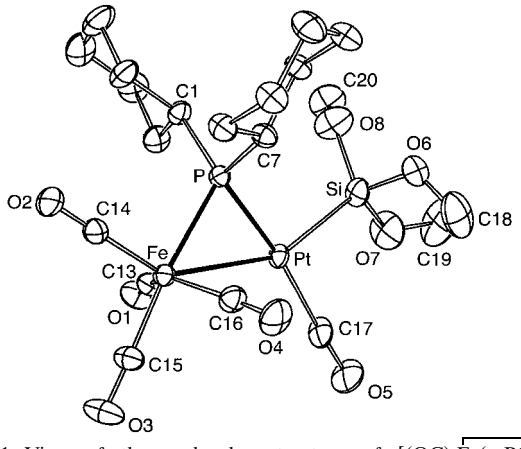

Figure 1. View of the molecular structure of $[(OC)_4\overline{Fe(\mu\text{-}PCy_2)}Pt\{Si(OMe)_3\}(CO)]$ (**2b**).

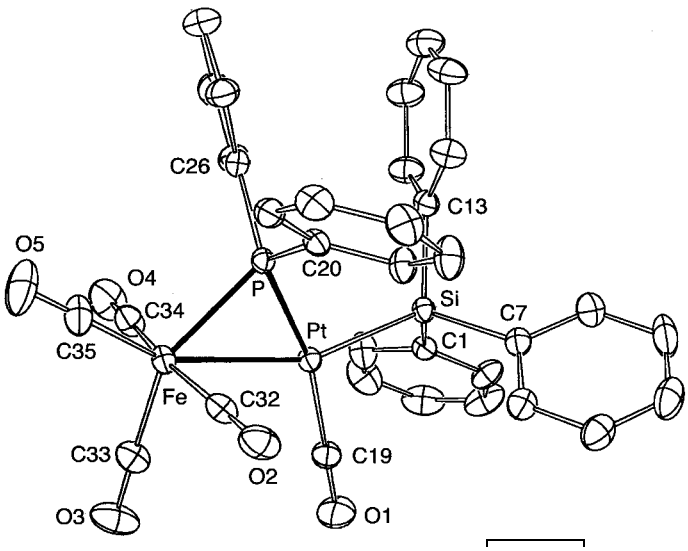

Figure 2. View of the molecular structure of $[(OC)_4\overline{Fe(\mu\text{-}PPh_2)}Pt(SiPh_3)(CO)]$ (**2c**).

The Pt–Si bond length in these complexes is similar to that found in the mononuclear complexes $[HPt(SiH_3)(PCy_3)_2]$ (238.2(3) pm),[24a] $[Pt(SiMe_2Ph)Cl(PMe_2Ph)_2]$ (229 pm),[1b] or $[PtH\{SiMe(CH_2SPh)_2\}(PPh_3)_2]$ (235.6(1) pm), but shorter than in $[Pt\{SiPh(SiMe_3)_2\}Cl(dcpe)]$ (242.3(2) pm).[24b,c] The value of the P-Pt-Si angle in **2b** (98.07(5)°) and **2c** (105.17(6)°) reflects the increasing steric bulk of the silyl

0947-6539/00/0623-4268 $ 17.50+.50/0 *Chem. Eur. J.* **2000**, *6*, No. 23

Table 2. Selected bond lengths [pm] and angles [°] in **2b**.

Fe–Pt	272.33(7)	Fe-P-Pt	73.28(3)
Fe–P	230.4(1)	P-Fe-Pt	52.59(3)
Pt–P	225.9(1)	P-Pt-Fe	54.13(3)
Fe–C13	181.8(6)	C14-Fe-C13	113.3(3)
Fe–C14	178.4(6)	C14-Fe-C16	110.2(3)
Fe–C15	177.8(6)	C13-Fe-C16	136.5(3)
Fe–C16	179.9(6)	P-Fe-C15	173.8(2)
Pt–C17	189.8(6)	P-Fe-C14	89.9(2)
Pt–Si	231.9(2)	P-Pt-Si	98.07(5)
Si–O6	161.4(5)	P-Pt-C17	167.3(2)
Si–O7	161.0(5)	Si-Pt-C17	92.7(2)
Si–O8	163.6(6)	Si-Pt-Fe	152.20(5)

Table 3. Selected bond lengths [pm] and angles [°] in **2c**.

Fe–Pt	271.76(9)	Fe-P-Pt	73.81(5)
Fe–P	227.5(2)	P-Fe-Pt	52.69(4)
Pt–P	225.1(2)	P-Pt-Fe	53.50(4)
Fe–C32	178.7(8)	C34-Fe-C35	96.3(4)
Fe–C33	179.2(8)	C32-Fe-C35	97.2(4)
Fe–C34	179.1(8)	C32-Fe-C34	166.3(4)
Fe–C35	178.4(8)	P-Fe-C33	149.1(2)
Pt–C19	189.9(7)	P-Fe-C35	102.6(3)
Pt–Si	236.4(2)	P-Pt-Si	105.17(6)
		P-Pt-C19	163.4(2)
		Si-Pt-C19	90.7(2)
		Si-Pt-Fe	157.98(5)

ligand. The Fe–Pt bond length in **2b** (272.33(7) pm) and **2c** (271.76(9) pm) is slightly longer than that in **1a** (259.40(7) pm). This may be related to the change in electron density in this bond that results from the ligand rearrangement observed. The position of the ν(CO) bands in the IR spectrum of these complexes is very similar to that of $[Fe(CO)_4(PPh_3)]$ in CH_2Cl_2 [2049 (vs), 1974 (m), 1938 cm^{-1} (vs)].[25] A splitting of the E vibration mode is due to a slight distorsion of the Fe moiety away from the C_{3v} symmetry found in $[Fe(CO)_4(PPh_3)]$. This similarity suggests that the metal–metal bonding in complexes **2a–e** should be better described as $Fe(d^8) \rightarrow Pt(d^8)$ with a formal dative bond between an Fe^0 and a Pt^{II} center [Scheme 3 (**I**)] although the alternative $Fe(d^7)-Pt(d^9)$ situation [Scheme 3 (**II**)] may also contribute to the actual bonding description of the complexes.

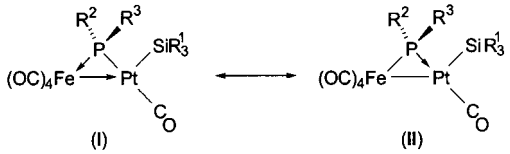

Scheme 3. Resonance forms for complexes **2a–e**.

When solutions of complexes **1a** or **1c** were slowly treated with two equivalents of *t*BuNC at low temperature, quantitative displacement of the COD ligand was observed and complexes **3a** and **3c** were isolated [Eq. (3)]. They are stable in solution for a few days and **3c** was characterized by X-ray diffraction. Silyl migration from Fe to Pt also occurred in these complexes and an isonitrile ligand is now bound to each metal center. The ν(CN) vibration of the Pt-bound isonitrile ligand is found at about 20 cm^{-1} higher than that of the Fe-bound isonitrile ligand, a trend similar to that observed with

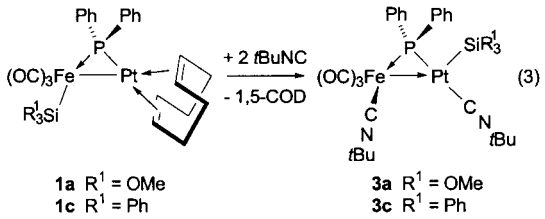

the CO ligands in **2a–e** that is due to a lower back-bonding ability of the Pt fragment.

A view of the molecular structure of **3c** is shown in Figure 3 and selected bond lengths and angles are given in Table 4. The $SiPh_3$ ligand is again *cis* with respect to the phosphido bridge,

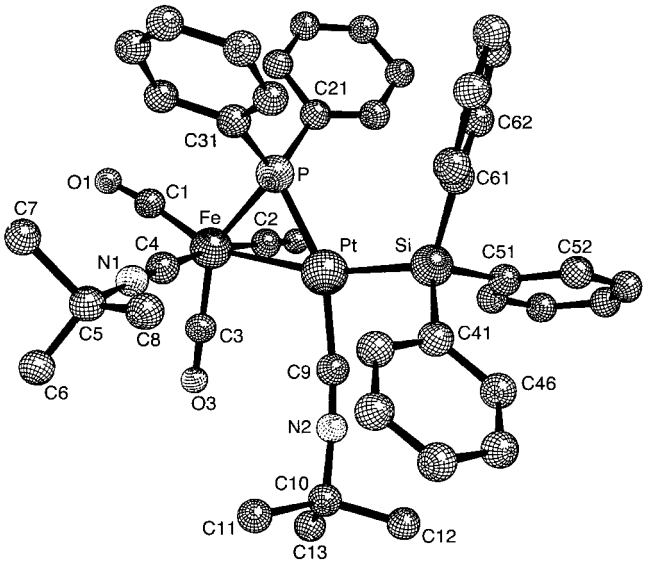

Figure 3. View of the molecular structure of $[(OC)_3(tBuNC)Fe(\mu\text{-}PPh_2)Pt\{SiPh_3\}(CNtBu)]$ (**3c**).

Table 4. Selected bond lengths [pm] and angles [°] in **3c**.

Fe–Pt	271.9(1)	Fe-P-Pt	74.64(7)
Fe–P	225.2(2)	P-Fe-Pt	52.36(6)
Pt–P	223.3(2)	P-Pt-Fe	53.00(6)
Fe–C1	176(1)	C1-Fe-C2	97.5(6)
Fe–C2	175(1)	C2-Fe-C4	165.3(5)
Fe–C3	178(1)	C1-Fe-C4	97.2(5)
Fe–C4	189(1)	C1-Fe-C3	109.7(4)
Pt–C9	195.7(9)	P-Fe-C1	104.6(4)
C4–N1	114(1)	P-Pt-Si	112.90(7)
N1–C5	146(1)	P-Pt-C9	157.7(2)
C9–N2	116(1)	Fe-C4-N1	177.5(8)
N2–C10	141(1)	C4-N1-C5	176(1)
Pt–Si	233.3(2)	Pt-C9-N2	172.9(8)
		C9-N2-C10	170.7(9)

while the (μ-P)-Pt-C9 angle involving the isonitrile ligand is 157.7(2)°. The isonitrile ligand bound to iron is orthogonal to the Fe-(μ-P)-Pt plane with a (μ-P)-Fe-C(4) angle of 88.7(3)°; this is likely to be due to steric reasons.

When complex **2b** was treated with one equivalent of *t*BuNC, selective substitution of the Pt-bound CO ligand was observed to give **4b**. The corresponding ν(CO) vibration around 2079 cm^{-1} in the precursor is replaced by a ν(CN)

absorption at 2179 cm^{-1}. Although the metal–metal bond in complexes **2a,b** was not opened by excess CO at one atmosphere, it readily did so in the presence of two equivalents of *t*BuNC to give the complexes $[(OC)_4Fe(\mu\text{-}PPh_2)Pt\{Si(OMe)_3\}(CN\textit{t}Bu)_2]$ (**5a**) (most likely via **4a** which was not observed) and $[(OC)_4Fe(\mu\text{-}PCy_2)Pt\{Si(OMe)_3\}(CN\textit{t}Bu)_2]$ (**5b**) in which the silyl ligand is now *trans* to the phosphido bridge (see below) [Eq. (4)]. Similarly, the Fe → Pt bond in **3a** was opened by *t*BuNC to give complex **6** [Eq. (5)].

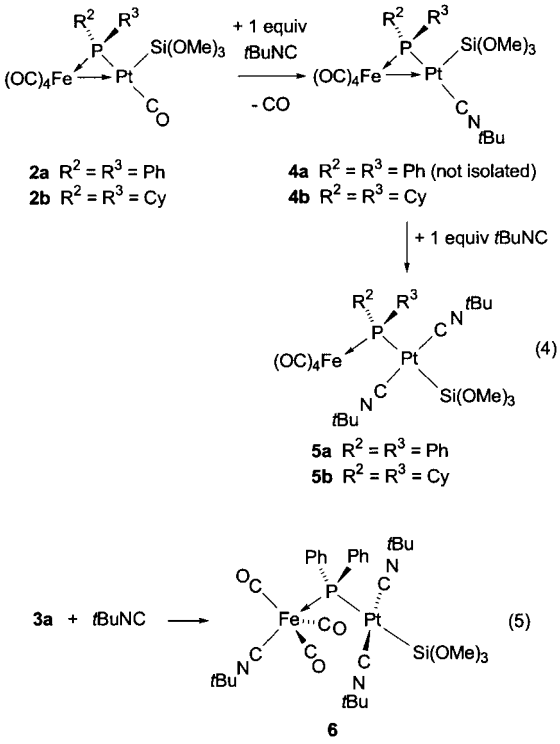

The easy opening of the metal–metal bond in these reactions is consistent with its formal dative character (vide supra). This is accompanied by a characteristic high-field shift of the $^{31}P\{^1H\}$ NMR resonance for the phosphido ligand and a decrease of the $^1J(P,Pt)$ coupling constant (ca. 1100 Hz). For comparison, the $^1J(P,Pt)$ coupling for the P atom *trans* to the silyl ligand is 1626 Hz in *cis*-$[Pt(SiHMe_2)_2(PEt_3)_2]$.[26] The $^{13}C\{^1H\}$ NMR resonance for the Pt-bound isonitrile carbon atoms in **5b** is observed at $\delta = 130.6$ with $^1J(C,Pt) = 1434$ Hz. These values are typical for such a ligand bound to platinum; in the Pt^0 cluster $[Pt_3(\mu\text{-}CN\textit{t}Bu)_3(CN\textit{t}Bu)_3]$ values of $\delta = 161.4$ and $^1J(C,Pt) = 1935$ Hz are found.[27] The isomerization observed for the silyl ligand from *cis* to μ-P in **2** or **3** to *trans* in **5** or **6** is noteworthy and was clearly established by an X-ray diffraction study of **6**. A view of the molecular structure is shown in Figure 4 and selected bond lengths and angles are given in Table 5.

The separation of 373.1(1) pm between the metals indicates complete opening of the metal–metal bond. The coordination geometry around the Fe center is trigonal bipyramidal and that around Pt is square planar. There is very little distorsion away from ideal geometries due to the widening of the Fe-(μ-P)-Pt angle (105.7(2)°). The Fe–P bond length (227.6(3) pm) is not significantly affected when compared to the other structures in this work, whereas a lengthening of the Pt–P bond length (240.3(4) pm) is observed. This is consistent with the *trans*-influence of the silyl ligand.

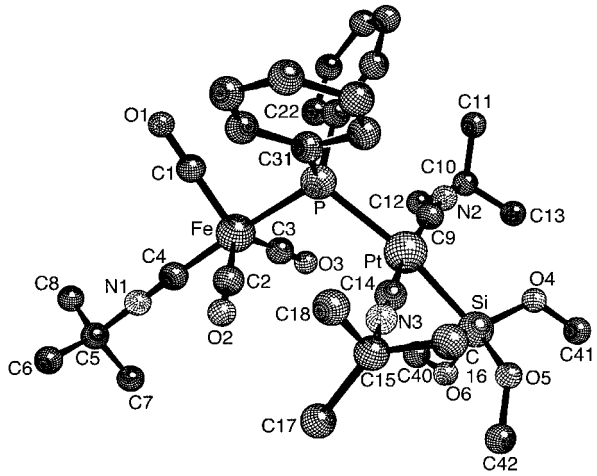

Figure 4. View of the molecular structure of $[(OC)_3(\textit{t}BuNC)Fe(\mu\text{-}PPh_2)Pt\{Si(OMe)_3\}(CN\textit{t}Bu)_2]$ (**6**).

Table 5. Selected bond lengths [pm] and angles [°] in **6**.

Fe–P	227.6(3)	Fe-P-Pt	105.7(2)
P–Pt	240.3(4)	P-Pt-Si	169.6(1)
Fe–C4	186(1)	P-Pt-C9	93.0(5)
C4–N1	114(2)	P-Pt-C14	92.7(4)
N1–C5	147(2)	C9-Pt-C14	172.5(5)
Pt–C9	199(1)	Pt-C14-N3	176(1)
C9–N2	112(1)	C14-N3-C15	177(1)
N2–C10	149(2)	Pt-C9-N2	177(1)
Pt–C14	200(1)	C9-N2-C10	172(1)
C14–N3	112(1)	P-Fe-C1	91.9(4)
N3–C15	150(2)	C1-Fe-C4	90.8(6)
Pt–Si	235.5(4)	Fe-C4-N1	178(1)
Si–O4	164.0(9)	C4-N1-C5	178(1)
Si–O5	164(1)	C1-Fe-C2	116.7(7)
Si–O6	163(1)	C1-Fe-C3	118.8(6)
		C2-Fe-C3	124.5(7)

Factors governing the silyl-migration reaction: In order to assess the inter- or intramolecular nature of this unprecedented silyl-migration reaction, the following cross-experiment was conducted. A mixture of complexes **1a** and **1d** was treated with carbon monoxide and the reaction monitored by $^{31}P\{^1H\}$ NMR spectroscopy (see Figure 5). The only products detected were **2a** and **2d**, respectively. This should be confidently taken as evidence for an *intramolecular* mechanism, that is, this silyl-migration reaction may be considered as an intramolecular redox rearrangement. In contrast, irreversible *intermolecular* silyl-transfer reactions have been reported with $[Hg(SiMe_3)_2]$[28a] or $[Cd(SiF_3)_2]$.[28b]

The fact that the Pt–Si bond is usually stronger than the Fe–Si bond[1a] probably explains the direction of the silyl migration, although a complete energetic balance must take into account the loss of a Pt–CO (or Pt–CNR) bond and the formation of a Fe–CO (or Fe–CNR) bond. Although a stepwise, nonconcerted mechanism cannot be strictly ruled out (see below, Scheme 5), it appears reasonable to suggest a concerted, dyotropic-type rearrangement for this reaction (a

0947-6539/00/0623-4270 $ 17.50+.50/0 *Chem. Eur. J.* **2000**, *6*, No. 23

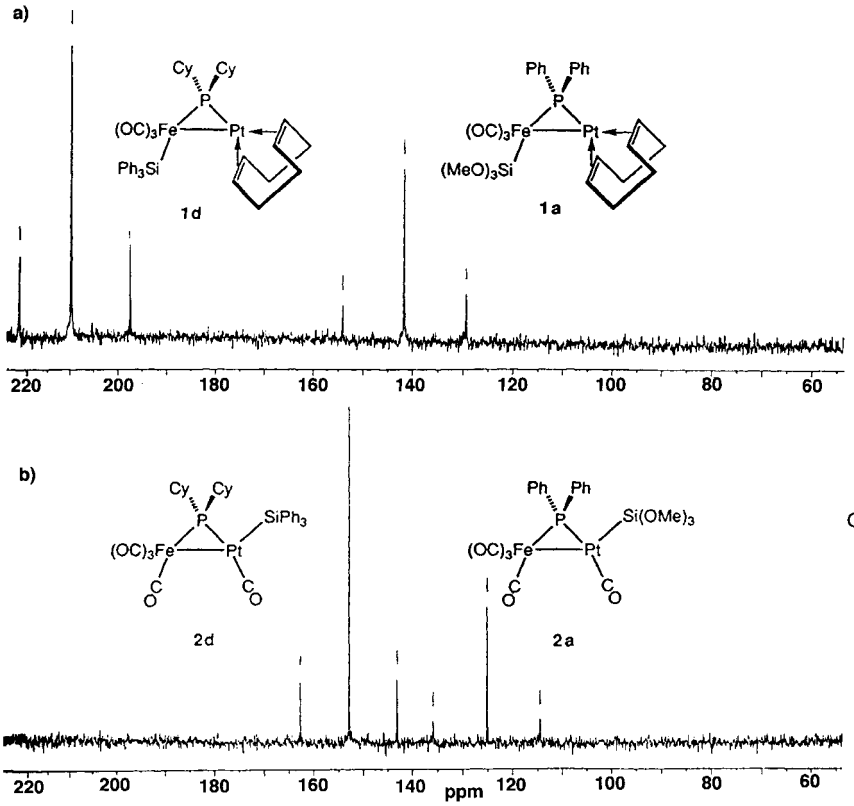

Figure 5. $^{31}P\{^1H\}$ NMR cross-over experiment between a) **1a** and **1d** yielding only b) **2a** and **2d**.

type of $[1,2]^2$-migration),[29] with an intermediate (or transition state) that involves a bridging silyl ligand (2e-3c bond) and a bridging carbonyl, or bridging isonitrile in the case of Equation (3), as depicted in **C** (Scheme 4). This species would

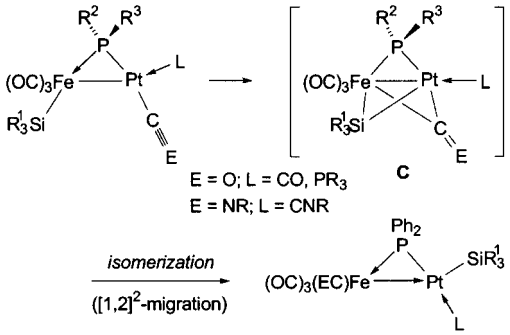

Scheme 4. Dyotropic-type concerted mechanism of silyl migration (see text).

then be isolobal with $[Fe_2(CO)_9]$. Although bridging silyl ligands have rarely been considered, this bonding situation has been structurally characterized in boranes,[30] in $Li(THF)_4[Cu_5Cl_4\{Si(SiMe_3)_3\}_2]$,[31] and very recently in $[(iPr_3P)Rh(H)(\mu\text{-}Cl)(\mu\text{-}SiPh_2)(\mu\text{-}SiPh_3)Rh(H)(PiPr_3)]$, which was prepared according to [Eq. (6)].[32]

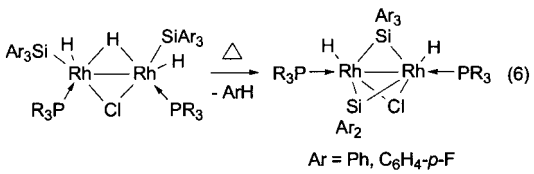

(6)

These last results nicely support our mechanistic considerations about the migration of silyl ligands from one metal to another. On the basis of NMR experiments, Akita et al.[33] and Girolami et al.[34] have independently concluded that the silyl ligand could reversibly flip from one metal center to another in dinuclear $SiMe_3$-substituted Ru–Ru complexes via a μ_2-SiR_3 intermediate [Eq. (7)]. However, no intermediate complex could be isolated.

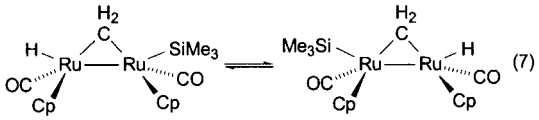

(7)

The dynamic behavior of Girolami's diruthenium complex was explained by reversible migration of the silyl group between the two Ru centers in the low-temperature regime [Eq. (8a)] and reversible migration to the bridging methylene group in the high-temperature dynamic process [Eq. (8b)].[34]

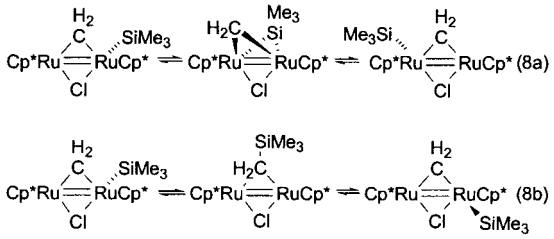

Recent studies with diruthenium complexes[33b] analogous to those in Equation (7) and with heteronuclear Mo–Re complexes[35] have shown that an $-SnMe_3$ or $-SnPh_3$ ligand, respectively, can also reversibly migrate from one metal to another.

Influence of the substituents at silicon: Whereas for **1a–e** the rates of the CO-induced 1,2-silyl-migration reaction leading to $[(OC)_4Fe(\mu\text{-}PR^2R^3)Pt(SiR^1_3)]$ (**2a–e**) [Eq. (2)] were too fast (irrespective of the stereoelectronic properties of the SiR^1_3 ligand or of the phosphido bridge) to allow detection of any intermediate (see above), the isomerization kinetics of $[(OC)_3(R^1_3Si)Fe(\mu\text{-}PPh_2)Pt(PPh_3)_2]$ (**7a–d**) was found to strongly depend on the substituents at silicon [Eq. (9)].

When CO was bubbled through a CH_2Cl_2 solution of $[(OC)_3\{(MeO)_3Si\}Fe(\mu\text{-}PPh_2)Pt(PPh_3)_2]$ (**7a**), the PPh_3 ligand *trans* to the phosphido bridge was stereoselectively and quantitatively substituted within ten minutes to afford **8a**. This species rearranged in solution within approximately 1 h to its isomer $[(OC)_4Fe(\mu\text{-}PPh_2)Pt\{Si(OMe)_3\}(PPh_3)]$ (**9a**).[11]

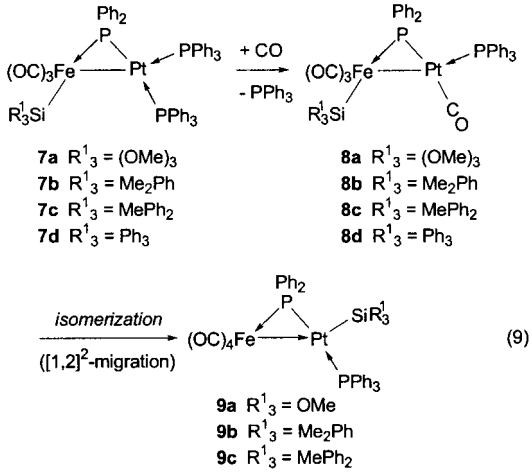

(9)

Similarly, when $[(OC)_3(PhMe_2Si)\overline{Fe(\mu\text{-}PPh_2)}\overline{Pt(PPh_3)_2}]$ (**7b**) was treated with CO, $[(OC)_3(PhMe_2Si)\overline{Fe(\mu\text{-}PPh_2)}\overline{Pt(CO)(PPh_3)}]$ (**8b**) was rapidly and quantitatively formed. It took, however, about 5 h for **8b** to isomerize to **9b**. The derivative **8c** could similarly be isolated in 83% yield after purging a solution of **7c** with CO, but the silyl migration leading to **9c** took three days for completion (monitored by IR and $^{31}P\{^1H\}$ NMR spectroscopy). The $SiPh_3$-substituted derivative **8d**, which has been structurally characterized,[22b] showed no tendency to rearrange, even after several days in solution. Therefore, for a given phosphido ligand, μ-PPh_2 in this series, the sequence of decreasing migration ability for the silyl ligand appears to be: $Si(OMe)_3 > SiMe_2Ph > SiMePh_2 \gg SiPh_3$. These findings demonstrate that the *steric* requirements of the SiR^1_3 group rather than the electronic properties of the substituents R^1 on silicon are decisive for the ease of silyl migration in these complexes. If electronic effects were dominating, one would expect a different trend: a $SiPh_3$ ligand bearing three electron-withdrawing phenyl groups is of course less electron withdrawing than an alkoxysilyl group, but more than a $SiMe_2Ph$. By analogy with the cone angle concept established for PR_3 ligands,[36] a $SiPh_3$ ligand evidently exhibits a significantly larger steric bulk than a $Si(OMe)_3$ or a $SiMe_2Ph$ group. Recall, however, that migration of an $SiPh_3$ ligand was described above [Eq. (3)].

Influence of the CO pressure: In order to qualitatively evaluate the influence of the CO pressure we monitored by IR (ν(CO) region) and $^{31}P\{^1H\}$ NMR spectroscopy the transformation of the $SiMePh_2$-substituted derivative **8c** in a steel autoclave at ambient temperature under a CO pressure of 45 atm. A significant rate enhancement was observed, since after 18 h about 90% of **8c** has been isomerized to **9c** and after 24 h no **8c** could be detected anymore, whereas three days were required under 1 atm of CO. Since displacement of the Pt-bound PPh_3 ligand *trans* to μ-P by CO is a very facile reaction, it is not this step that is rate-controlling and on which CO pressure would have made such a difference. If the silyl-migration reaction was to occur in a stepwise manner, as shown in Scheme 5, in contrast to the concerted mechanism discussed above, one would expect the 16e Fe center of the first intermediate that results from formal reductive elimination to readily coordinate CO under pressure to give the coordinatively saturated product $[(OC)_4Fe(\mu\text{-}PPh_2)Pt(SiMePh_2)(CO)(PPh_3)]$ (see below the transformation of **7e** to **10** [Eq. (10)]). This was not observed during the $^{31}P\{^1H\}$ NMR monitoring. Furthermore, CO pressure would also be expected to slow down or completely prevent decoordination of CO from Pt, which represents a required step for the formation of the metal–metal bond in **9c**. We therefore believe that the concerted, dyotropic-type mechanism suggested above in Scheme 4 is the most likely.

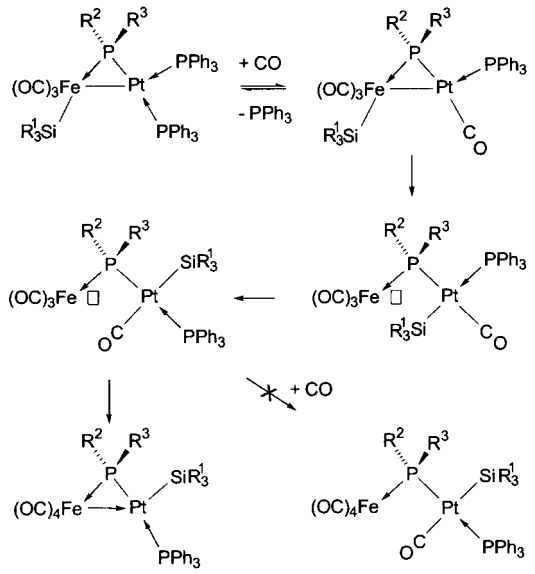

Scheme 5. Alternative mechanism involving stepwise silyl migration (see text).

Influence of the phosphido group: The reactivity of the complexes $[(OC)_3(R^1_3Si)\overline{Fe(\mu\text{-}PR^2R^3)}\overline{Pt(PPh_3)_2}]$ is furthermore influenced by the substituents at the phosphido bridge. After purging a CH_2Cl_2 solution of **7e** [^{29}Si NMR: $\delta = 10.2$ (dd, $^2J(P,Si) = 40$ Hz, $^3J(P,Si) = 15$ Hz] with CO for approximately 50 min, monitoring by IR and $^{31}P\{^1H\}$ NMR spectroscopy revealed that the PPh_3 ligand *trans* to the μ-PHCy bridge was again selectively substituted to afford **8e** [Eq. (10)].

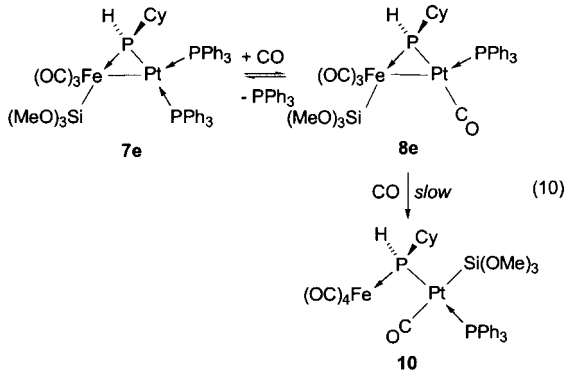

(10)

The proton-coupled ^{31}P NMR spectrum of **8e** consisted of a doublet at $\delta = 146.7$ with a $^1J(P,H)$ coupling of 363 Hz ($^1J(Pt,P) = 2290$ Hz) and a broadened singlet at $\delta = 27.6$

0947-6539/00/0623-4272 $ 17.50+.50/0 *Chem. Eur. J.* **2000**, *6*, No. 23

assigned to the PPh_3 ligand *cis* to the phosphido bridge ($^1J(Pt,P) = 3110$ Hz). The presence of the liberated PPh_3 was confirmed by the observation of a broad signal at $\delta = -4.3$. In contrast to the stable derivatives **8a–d**, the platinum-bound carbonyl ligand of **8e** [$\nu(CO) = 2047$ cm^{-1} (s)] was reversibly replaced by PPh_3 after concentration of the solution under reduced pressure, thus regenerating **7e**. We therefore did not succeed in isolating **8e** in pure form. However, when a solution of **8e** was purged for several hours with a gentle stream of CO, transfer of the $Si(OMe)_3$ ligand from iron to platinum, cleavage of the metal–metal bond and coordination of a carbonyl ligand on iron gradually occurred [Eq. (10)]. The ligand arrangement in the dinuclear silyl complex **10** was deduced from multinuclear NMR studies. Characteristic for a dinuclear μ-PR_2 complex without a metal–metal bond, the phosphido signal at $\delta = 70.6$ is drastically shifted to high field relative to those of **7e** ($\delta = 169.4$) or **8e** ($\delta = 146.7$). In contrast to **5a,b** which have the silyl group *trans* to μ-PR_2, the $Si(OMe)_3$ group in **10** is *cis* to both the bridge and the PPh_3 ligand ($\delta = 36.4$, $^1J(Pt,P) = 3073$ Hz) and whose large $^2J(P,P)$ coupling of 283 Hz is diagnostic for the *trans*-P-Pt-P arrangement. The high-field shift of the signal centered at $\delta = -24.9$ in the ^{29}Si INEPT NMR spectrum of **10** confirms the migration of the alkoxysilyl ligand from iron to platinum ($^1J(Pt,Si) = 2523$ Hz), and the small $^2J(P,Si)$ coupling of 15 Hz (most likely with the PPh_3 ligand as coupling with μ-P is very small) is also in accordance with the structure drawn. The presence of a Pt–Si bond leads to the observation of a $^3J(Pt,C)$ coupling of 19 Hz for the $Si(OMe)_3$ signal. As known for mononuclear iron complexes of the type $[Fe(CO)_4(PR_3)]$,[25] the four carbonyl ligands of the iron moiety of **10** are fluxional at ambient temperature and give rise to a doublet at $\delta = 210.2$, due to a $^2J(P,C)$ coupling of 13 Hz. Despite of a long data-acquisition time, we could not detect any signal due to the Pt-bound carbonyl ligand in the anticipated δ 180–190 region. The presence of a Pt-bound carbonyl ligand is, however, inferred unambiguously from the IR spectrum, which displays, in addition to four $\nu(CO)$ stretches [2004 (w), 1975 (s), 1952 (s), 1929 cm^{-1} (s)] stemming from the $Fe(CO)_4$ moiety, a fifth intense vibration at 2042 cm^{-1}.

The much more difficult silyl-migration reaction in complexes with a μ-PHCy bridge as opposed to μ-PPh_2, under similar conditions, could be explained by invoking the Thorpe–Ingold effect.[37] Bulkier geminal substituents on the μ-P atom would promote the formation of transition-state or intermediate structures that contain additional bridging ligands and thus facilitate their transfer from one metal to the other. The deviating behavior of μ-PRH heterobimetallics as opposed to their μ-PR_2 analogues has also been noted in compounds of the type $[(OC)_5M(\mu\text{-}PRH)Pt(H)(PPh_3)_2]$ (M = Cr, Mo, W; R = Ph, Cy), which could not be converted to the metal–metal-bonded complexes $[(OC)_4M(\mu\text{-}PRH)Pt(\mu\text{-}H)(PPh_3)]$ by dissociation of a CO and a PPh_3 ligand,[16a] a reaction well documented for $[(OC)_5M(\mu\text{-}PPh_2)Pt(H)(PPh_3)_2]$.[15b] The Thorpe–Ingold effect has also been put forward to explain the suppression of intramolecular, intermetal transfer of CO in heteronuclear complexes of the type $[M(\mu\text{-}PR_2)Pt]$ on going from μ-PR_2 to μ-PRH systems.[38]

Influence of the nature of the added nucleophile: In order to explore further the scope of donor ligands that promote this unusual silyl-migration reaction, we reacted **1c** with two equivalents of the phosphites $P(OMe)_3$ or $P(OPh)_3$, or of the functional phosphine $Ph_2PCH_2C(O)Ph$ in CH_2Cl_2 or toluene. Complexes **11a–c** were rapidly formed in almost quantitative yield and have been fully characterized [Eq. (11)].[22a,c]

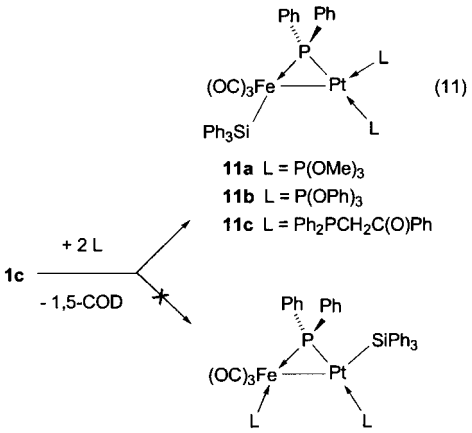

No silyl-migration reaction was observed in these cases, whereas addition of two equivalents of *t*BuNC to **1a** or **1c** yielded the products of 1,2-silyl migration **3a** and **3c**, respectively [Eq. (3)]. Substitution of one of the PPh_3 ligands of $[(OC)_3(Ph_3Si)Fe(\mu\text{-}PPh_2)Pt(PPh_3)_2]$ (**7d**) by PMe_3 occurred stereoselectively, since only the PPh_3 ligand *trans* to the phosphido bridge was substituted.[22a] The reaction of **7a–d** with CO first led to $[(OC)_3(R^1Si)Fe(\mu\text{-}PPh_2)Pt(CO)(PPh_3)]$ (**8a–d**), with again selective substitution of the phosphine *trans* to the μ-P atom, which then isomerized in the case of **8a–c** to $[(OC)_4Fe(\mu\text{-}PPh_2)Pt(SiR^1_3)(PPh_3)]$ (**9a–c**) [Eq. (9)].[11]

The reaction of $[(OC)_3(R^1_3Si)Fe(\mu\text{-}PR^2R^3)Pt(PPh_3)_2]$ with slightly more than one equivalent of *t*BuNC in CH_2Cl_2 at ambient temperature afforded within 15 minutes the yellow stable compounds $[(OC)_3(R^1_3Si)Fe(\mu\text{-}PR^2R^3)Pt(PPh_3)(CN\textit{t}Bu)]$ (**12a–c**) in almost quantitative spectroscopic yield, irrespective of the nature of the SiR^1_3 and μ-PR^2R^3 ligands [Eq. (12)]. Monitoring the reaction of **7a** by $^{31}P\{^1H\}$ NMR spectroscopy in a NMR tube over several hours, even in the presence of 2.5 equivalents of *t*BuNC, showed no evidence for substitution of the remaining PPh_3 ligand, opening of the metal–metal bond, or for silyl migration. A comparison of these results with the behavior of **8a–d** [Eq. (9)] shows that a phosphine ligand bound to Pt (*cis* to μ-P) significantly slows down silyl migration relative to CO, as in the assumed intermediate of Equation (2). Whereas silyl migration is still possible when CO is bound to Pt, complete inhibition of the reaction is caused by this phosphine when an isonitrile ligand is also bound to Pt, as in **12a–f**.

Reaction of $[(OC)_3\{(MeO)_3Si\}Fe(\mu\text{-}PHCy)Pt(PPh_3)_2]$ (**7e**) with two equivalents of 2,6-dimethylphenyl isonitrile, a better π-acceptor ligand than *t*BuNC, also exclusively yielded the monosubstitution product $[(OC)_3\{(MeO)_3Si\}Fe(\mu\text{-}PHCy)Pt(PPh_3)(CNxylyl)]$ (**12d**). The selective substi-

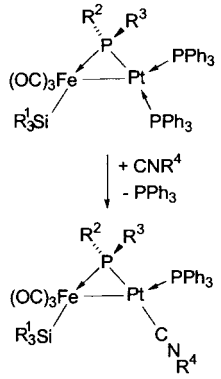

(12)

12a R^1_3 = $(OMe)_3$, R^2 = Ph, R^3 = Ph, R^4 = *t*Bu
12b R^1_3 = $(OMe)_3$, R^2 = H, R^3 = Cy, R^4 = *t*Bu
12c R^1_3 = $(MePh_2)$, R^2 = Ph, R^3 = Ph, R^4 = *t*Bu
12d R^1_3 = $(OMe)_3$, R^2 = H, R^3 = Cy, R^4 = xylyl
12e R^1_3 = (Me_2Ph), R^2 = Ph, R^3 = Ph, R^4 = xylyl
12f R^1_3 = Ph_3, R^2 = Ph, R^3 = Ph, R^4 = xylyl

tution of the PPh_3 ligand *trans* to the phosphido bridge and the conservation of the metal–metal bond in derivatives **12a–f** were deduced from the $^{31}P\{^1H\}$ NMR spectra, which exhibited a weakly coupled doublet resonance in the $\delta = 140-150$ region due to the μ-PR_2 ligand and a second doublet in the $\delta = 27-28$ region due to the PPh_3 ligand in relative *cis* orientation to the bridge. Both resonances were flanked by ^{195}Pt satellites with large ^1J(Pt,P) couplings (Table 1). The spectroscopic data obtained in solution for complexes **12a–f** are consistent with the results of an X-ray diffraction study of **12f**. A view of the molecular structure is shown in Figure 6 and a perspective view along the Fe–Pt axis showing the core structure is given in Figure 7. Selected bond lengths and angles for compound **12f** are given in Table 6.

The general structural features are very similiar to those obtained for $[(OC)_3(Ph_3Si)Fe(\mu\text{-}PPh_2)Pt(CO)(PPh_3)]$ (**8d**).[22b] As in the latter complex (Fe–Pt = 262.0(1) pm), the Fe–Pt separation of 263(1) pm is noticeably shorter than

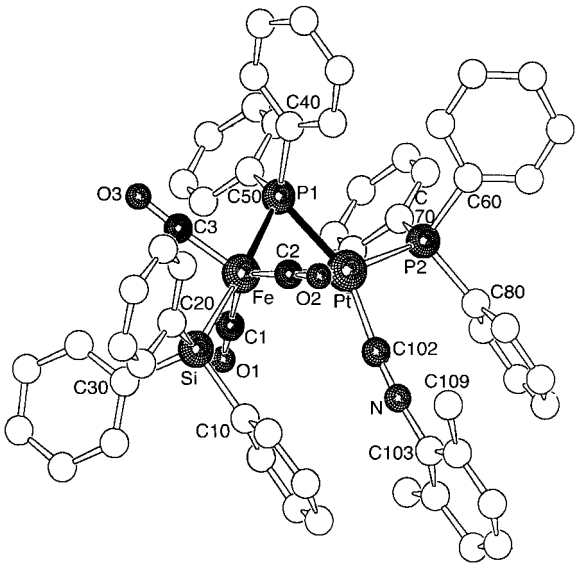

Figure 6. View of the molecular structure of $[(OC)_3(Ph_3Si)Fe(\mu\text{-}PPh_2)Pt(PPh_3)(CNxylyl)]$ (**12f**) (the Fe–Pt bond is masked).

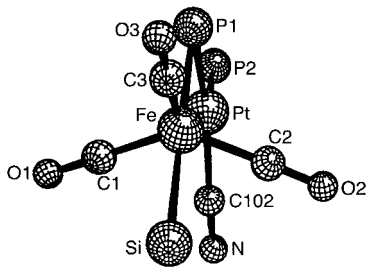

Figure 7. Perspective view of the core structure of $[(OC)_3(Ph_3Si)Fe(\mu\text{-}PPh_2)Pt(PPh_3)(CNxylyl)]$ (**12f**) along the Fe–Pt axis.

Table 6. Selected bond lengths [pm] and angles [°] in **12f**.

Fe–Pt	263.1(1)	Fe-P1-Pt	72.24(7)
Fe–P1	220.0(2)	C40-P1-C50	104.2(4)
Pt–P1	226.2(2)	P1-Pt-P2	107.78(8)
Pt–P2	227.8(2)	P1-Pt-C102	154.4(3)
Fe–C1	176.7(9)	P2-Pt-C102	97.6(3)
Fe–C2	177.9(9)	P1-Pt-Fe	159.88(6)
Fe–C3	176(1)	Fe-Pt-C102	101.78(8)
Fe–Si	233.1(2)	P1-Fe-Si	175.1(1)
Pt–C102	196.2(9)	Pt-Fe-Si	129.55(8)
N–C102	116(1)	Pt-Fe-P1	54.96(6)
N–C103	139(1)	Pt-Fe-C1	81.5(3)
		Pt-Fe-C2	75.9(3)
		Pt-Fe-C3	142.0(3)
		C1-Fe-C2	132.2(4)
		C2-Fe-C3	112.5(4)
		C1-Fe-C3	111.3(4)

those in **2b,c** and **3c** (ca. 272 pm), consistent with a formally rather covalent metal-metal bond. The phosphido bridge and the $SiPh_3$ group are in mutual *trans* position (P1-Fe-Si 175.1(1)°), and the three carbonyls on iron have a meridional arrangement. The coordination around Pt may be considered as distorted square planar (see Figure 6). The P1-Pt-C102 angle of 154.4(3)° between the isonitrile ligand and the μ-PPh_2 ligand deviates considerably from the ideal *trans* orientation, which may be a consequence, at least in part, of the steric bulk of the PPh_3 ligand (P2-Pt-C102 = 97.6(3)°). There is a small deviation from linear isonitrile ligation, the Pt-C102-N angle being 174.9(8)°. The Pt–C102 bond length of 196.2(9) pm is somewhat longer than that of the Pt–C bond of $[(OC)_3(Ph_3Si)Fe(\mu\text{-}PPh_2)Pt(CO)(PPh_3)]$ (**8d**; 191.6(6) pm), which reflects the less pronounced π-acceptor ability of the xylylisonitrile ligand compared to CO. The Fe–Si, Fe–P1, Pt–P1, and Pt–P2 bond lengths of 233.1(2), 220.0(2), 226.2(2), and 227.8(2) pm compare well with those found for **8d** (233.9(2), 219.6(2), 227.7(1), and 229.4(1) pm, respectively).

Finally, we note that complex **1a** in CH_2Cl_2 did not react with PhC≡CH, PhC≡CPh, or MeO(O)CC≡CC(O)OMe at 20 °C even after 12 h. A similar behavior was observed for **7a**.

Conclusion

We have described a family of phosphido-bridged bimetallic Fe–Pt complexes that gives rise to unprecedented, intramolecular transformations involving 1,2-migration of a silyl ligand from Fe to Pt with concomittant 1,2-migration of CO

0947-6539/00/0623-4274 $ 17.50+.50/0 *Chem. Eur. J.* **2000**, *6*, No. 23

(or in some cases CNR) from Pt to Fe. We investigated the influence of various parameters on this reaction, such as the nature of the substituents on the silyl ligand or on the phosphido bridge and that of the external nucleophile that triggers this dyotropic-type rearrangement. We have found that CO or CNR ligands are capable of promoting this silyl migration, as opposed to phosphines or phosphites. Isonitriles or CO can also lead to substitution reactions at Fe or open the metal–metal bond. Our results show that relatively minor changes in substituents are sufficient to completely modify the reactivity of the bimetallic complexes. Our recent observation that an iron-to-platinum silyl migration may also occur in bis-dppm-bridged Fe–Pt complexes[39] suggests that silyl migration from one metal to another, a process that could have implications in the metal-catalyzed silicon chemistry, may occur more easily than previously thought owing to the small energy changes involved.

Experimental Section

All reactions were performed in Schlenk-tube flasks under purified nitrogen. Solvents were dried and distilled under nitrogen before use: toluene, pentane and hexane over sodium, dichloromethane from P_4O_{10}. Nitrogen was passed through BASF R3–11 catalyst and molecular sieve columns to remove residual oxygen or water. Elemental C, H and N analyses were performed on a Leco Elemental Analyser CHN 900. Infrared spectra were recorded in the 4000–400 cm^{-1} region on Bruker IFS 66 spectrometer. The ^1H, $^{31}P\{^1H\}$ and $^{13}C\{^1H\}$ NMR spectra were recorded at 200.13, 81.01, and 50.32 MHz, respectively, on a Bruker ACP 200 instrument and at 300.13, 121.50 and 75.48 MHz, respectively, on a Bruker AC 300 instrument. Phosphorus chemical shifts were externally referenced to 85% H_3PO_4 in H_2O, with downfield shifts reported as positive. ^{29}Si chemical shifts were measured on a Bruker ACP 200 instrument (39.76 MHz) and externally referenced to TMS, with downfield chemical shifts reported as positive. NMR spectra were recorded in pure $CDCl_3$, unless otherwise stated. The presence of CH_2Cl_2 of solvation in **9c** has been determined from the ^1H NMR spectrum. The reactions were generally monitored by IR spectroscopy in the ν(CO) region. 2,6-Xylylisonitrile and *tert*-butylisonitrile were obtained from Fluka and Aldrich and used as received. The following complexes were prepared as described in the literature: **1a–e**,[22a] **7a–e**,[22b] **8a**,**b**,[11] **8d**,[22b] **9a**,**b**,[11] **11a**,**b**,[22a] and **11c**.[22c]

[(OC)$_4$Fe(μ-PPh$_2$)Pt{Si(OMe)$_3$}(CO)] (2a): CO was slowly bubbled through a solution of complex **1a** (0.2 mmol) in CH_2Cl_2 (5 mL) at ambient temperature. Monitoring by IR and ^{31}P NMR spectroscopy indicated a complete conversion after a few seconds. After removal of all volatiles under reduced pressure, an orange oil, which is very soluble in pentane, was obtained. The spectroscopic yield is quantitative. Compound **2a** is stable in CO-saturated solution, but any attempt of isolation leads to degradation. ^1H NMR (200.13 MHz, $CDCl_3$): $\delta = 7.82-7.26$ (m, 10H; phenyl), 3.45 (s, $^4J(Pt,H) = 2.7$ Hz, 9H; $Si(OMe)_3$); $^{13}C\{^1H\}$ NMR (100.62 MHz, C_6D_6): $\delta =$ 207.8 (d, $^2J(P,C) = 11$ Hz, $^2J(Pt,C) = 32$ Hz, FeCO), 198.0 (brs, PtCO), 134.5–128.5 (m, phenyl), 50.1 (s, $^3J(Pt,C) = 12$ Hz, SiOMe); ^{29}Si NMR (C_6D_6): $\delta = -26.8$ (d, $^2J(P,Si) = 4$ Hz, $^1J(Pt,Si) = 2117$ Hz).

[(OC)$_4$Fe(μ-PCy$_2$)Pt{Si(OMe)$_3$}(CO)] (2b): Preparation analogous to **2a**; orange crystals, obtained from **1b**, were highly soluble in cyclohexane; the spectroscopic yield was quantitative. The product was very soluble in pentane and could be recrystallized from a concentrated pentane solution at −20 °C to afford single crystals suitable for X-ray analysis. Elemental analysis calcd (%) for $C_{20}H_{31}FeO_8PPtSi$ (709.45): C 33.86, H 4.40; found C 34.41, H 4.48; ^1H NMR (200.13 MHz, $CDCl_3$): $\delta = 3.56$ (s, $^4J(Pt,H) =$ 3.0 Hz, 9H; SiOMe), 2.30–0.85 (m, 22H; Cy); $^{13}C\{^1H\}$ NMR (100.62 MHz, C_6D_6): $\delta = 208.4$ (d, $^2J(P,C) = 11$ Hz, $^2J(Pt,C) = 37$ Hz, Fe-CO), 196.0 (brs, PtCO), 50.0 (s, $^3J(Pt,C) = 19$ Hz, SiOMe), 39.3 (d, $^1J(P,C) = 39$, $^2J(Pt,C) = 49$ Hz, Cy, C(P)), 33.1–32.5 (m, Cy, C_{ortho}), 27.8–27.6 (m, Cy, C_{meta}), 25.9 (s, Cy, C_{para}).

[(OC)$_4$Fe(μ-PPh$_2$)Pt(SiPh$_3$)(CO)] (2c): Preparation analogous to **2a**; orange crystals, obtained from **1c**, were highly soluble in pentane or hexane; the yield was spectroscopically quantitative. Compound **2c** could be recrystallized from a concentrated pentane/cyclohexane solution at −20 °C to afford orange single crystals suitable for X-ray analysis. Elemental analysis calcd (%) for $C_{35}H_{25}FeO_5PPtSi$ (835.59): C 50.31, H 3.02; found C 50.07, H 3.15; ^1H NMR (200.13 MHz, $CDCl_3$): $\delta = 7.49-7.11$ (m, phenyl).

[(OC)$_4$Fe(μ-PCy$_2$)Pt(SiPh$_3$)(CO)] (2d): Preparation analogous to **2a**; deep orange oil, obtained from **1d**, was highly soluble in pentane; the spectroscopic yield was quantitative. Compound **2d** was stable in CO-saturated solution, but attempts of isolation led to degradation. ^1H NMR (300.13 MHz, $CDCl_3$): $\delta = 7.59-7.32$ (m, 15H; phenyl), 1.83–0.88 (m, 22H; Cy).

[(OC)$_4$Fe(μ-PHPh)Pt(SiPh$_3$)(CO)] (2e): Preparation analogous to **2a**; deep orange oil, obtained from **1e**, was highly soluble in pentane; the spectroscopic yield was quantitative. Compound **2e** was stable in CO-saturated solution, but any attempt of isolation leads to degradation. ^1H NMR (300.13 MHz, $CDCl_3$): $\delta = 7.70-7.12$ (m, 20H; phenyl), 5.25 (d, $^1J(P,H) = 397.5$, $^2J(Pt,H) = 93.7$ Hz, PH).

[(OC)$_3$(*t*BuNC)Fe(μ-PPh$_2$)Pt{Si(OMe)$_3$}(CN*t*Bu)] (3a): *tert*-Butyl isonitrile (27 mg, 0.32 mmol) was added to a solution of **1a** (120 mg, 0.16 mmol) in CH_2Cl_2 (5 mL). After the mixture was stirred for 15 min, the yellow solution was concentrated under reduced pressure to about 1 mL and the orange product was precipitated by addition of pentane. Yield: 110 mg, 0.14 mmol, 85%; m.p. 89 °C; elemental analysis calcd (%) for $C_{28}H_{37}FeN_2O_6PPtSi$ (807.60): C 41.64, H 4.62, N 3.67; found C 41.90, H 4.68, N 3.44; ^1H NMR (300.13 MHz, $CDCl_3$): $\delta = 7.87-7.26$ (m, 10H; phenyl), 3.48 (s, 9H; SiOMe), 1.61 (s, 9H; PtCN*t*Bu), 0.91 (s, 9H; FeCN*t*Bu).

[(OC)$_3$(*t*BuNC)Fe(μ-PPh$_2$)Pt{SiPh$_3$}(CN*t*Bu)] (3c): Compound **3c** was prepared as described for **3a** from **1c** (140 mg, 0.16 mmol) in CH_2Cl_2 (5 mL). Yield: 130 mg, 0.14 mmol, 87%; orange powder; m.p. 96 °C; elemental analysis calcd (%) for $C_{43}H_{43}FeN_2O_3PPtSi$ (945.82): C 54.61, H 4.58, N 2.96; found C 54.23, H 4.50, N 2.84; ^1H NMR (200.13 MHz, $CDCl_3$): $\delta = 7.54-7.01$ (m, 25H; phenyl), 1.18 (s, 9H; PtCN*t*Bu), 0.95 (s, 9H; FeCN*t*Bu).

[(OC)$_4$Fe(μ-PCy$_2$)Pt{Si(OMe)$_3$}(CN*t*Bu)] (4b): Compound **4b** was prepared from **2b** (160 mg, 0.21 mmol) in CH_2Cl_2 (6 mL) by addition of one equivalent of *tert*-butyl isonitrile at ambient temperature. Yield: 130 mg, 0.17 mmol, 81%; orange powder; m.p. 88 °C; elemental analysis calcd (%) for $C_{24}H_{40}FeNO_7PPtSi$ (764.57): C 37.70, H 5.27, N 1.83; found C 37.84, H 5.27, N 1.80; ^1H NMR (300.13 MHz, $CDCl_3$): $\delta = 3.52$ (s, 9H; SiOMe), 2.38–1.65 (m, 16H; Cy), 1.59 (s, 9H; PtCN*t*Bu), 1.41–0.85 (m, 6H; Cy); $^{13}C\{^1H\}$ NMR (75.47 MHz, C_6D_6): $\delta = 210.5$ (d, $^2J(P,C) = 12$ Hz, $^2J(Pt,C) =$ 38 Hz, FeCO), 49.8 (s, $^3J(Pt,C) = 19$ Hz, SiOMe), 38.5 (d, $^1J(P,C) = 20$ Hz, $^2J(Pt,C) = 54$ Hz, C_{ipso}, Cy), 32.9–32.3 (m, C_{ortho}, Cy), 30.1 (s, *t*Bu), 27.7–27.6 (m, C_{meta}, Cy), 26.1 (s, C_{para}, Cy).

[(OC)$_4$Fe(μ-PPh$_2$)Pt{Si(OMe)$_3$}(CN*t*Bu)$_2$] (5a): Compound **5a** was prepared from **2a** (110 mg, 0.15 mmol) in CH_2Cl_2 (5 mL) by addition of two equivalents of *tert*-butyl isonitrile. Yield: 95 mg, 0.11 mmol, 78%; orange powder; m.p. 102 °C; elemental analysis calcd (%) for $C_{29}H_{37}FeN_2O_7PPtSi$ (835.61): C 41.68, H 4.46, N 3.35; found C 41.83, H 4.55, N 3.38; ^1H NMR (300.13 MHz, $CDCl_3$): $\delta = 7.78-7.20$ (m, 10H; Ph), 3.55 (s, 9H; SiOMe), 1.22 (s, 18H; CN*t*Bu).

[(OC)$_4$Fe(μ-PCy$_2$)Pt{Si(OMe)$_3$}(CN*t*Bu)$_2$] (5b): Compound **5b** was prepared from **2b** (180 mg, 0.24 mmol) in CH_2Cl_2 (5 mL) by addition of two equivalents of *t*butyl isonitrile. Yield: 170 mg, 0.20 mmol, 85%; orange powder; m.p. 112 °C; elemental analysis calcd (%) for $C_{29}H_{49}FeN_2O_7PPtSi$ (847.71): C 41.09, H 5.83, N 3.31; found C 40.89, H 5.83, N 3.20; ^1H NMR (300.13 MHz, $CDCl_3$): $\delta = 3.54$ (s, 9H; SiOMe), 2.31–1.68 (m, 16H; Cy), 1.55 (s, 18H; CN*t*Bu), 1.44–0.86 (m, 6H; Cy); $^{13}C\{^1H\}$ NMR (75.47 MHz, C_6D_6): $\delta = 216.9$ (d, $^2J(P,C) = 28$ Hz, CO), 210.5 (brs, CO), 130.6 (br m, $^1J(Pt,C) = 1434$ Hz, (Pt)C), 49.5 (s, SiOMe), 42.9 (s, C_{ipso}, Cy), 34.1–33.4 (m, C_{ortho}, Cy), 29.5 (s, *t*Bu), 28.4–28.0 (m, C_{meta}, Cy), 26.6 (s, C_{para}, Cy).

[(OC)$_3$(*t*BuNC)Fe(μ-PPh$_2$)Pt{Si(OMe)$_3$}(CN*t*Bu)$_2$] (6): Compound **6** was prepared from **3a** (90 mg, 0.12 mmol) in CH_2Cl_2 (5 mL) by addition of one equivalents of *tert*-butyl isonitrile at ambient temperature. Yield: 95 mg, 0.11 mmol, 89%; orange powder; m.p. 102 °C; elemental analysis calcd (%) for $C_{33}H_{46}FeN_3O_6PPtSi$ (890.73): C 44.50, H 5.21, N 4.72; found C 44.68, H 5.38, N 4.78; ^1H NMR (300.13 MHz, $CDCl_3$): $\delta = 7.85-7.24$ (m, 10H;

phenyl), 3.55 (s, 9H; SiOMe), 1.40 (s, 9H; FeCN*t*Bu), 1.18 (s, 18H; PtCN*t*Bu).

[(OC)$_3$(Ph$_2$MeSi)Fe(μ-PPh$_2$)Pt(PPh$_3$)(CO)] (8c): CO was bubbled for 10 min through a solution of **7c** (1170 mg, 1.0 mmol) in CH_2Cl_2 (30 mL). After completion of the reaction (monitored by IR and ^{31}P NMR spectroscopy), the solution was concentrated to about 5 mL and layered with Et_2O. After 24 h at $-30\,^{\circ}C$ a yellow powder precipitated, which was filtered, washed with pentane (15 mL), and then dried under vacuum. Yield: 840 mg, 83%; elemental analysis calcd (%) for $C_{47}H_{38}FeO_4P_2PtSi$ (1007.78): C 56.02, H 3.80; found C 56.23, H 4.04; ^{1}H NMR (200 MHz, C_6D_6): $\delta = 6.98-7.83$ (m, 35H; phenyl), 1.18 (s, 3H; SiMe).

[(OC)$_4$Fe(μ-PPh$_2$)Pt(SiMePh$_2$)(PPh$_3$)] (9c): CO was bubbled for 1 h through a solution of **7c** (234 mg, 0.2 mmol) in CH_2Cl_2 (10 mL). The reaction mixture was kept under a CO atmosphere for 3 d and the rearrangement from **8c** to **9c** was monitored by IR and ^{31}P NMR spectroscopy. After completion of the silyl migration, the solvent was evaporated, and the residue rinsed with Et_2O to remove PPh_3. Recrystallization from CH_2Cl_2/hexane at $-30\,^{\circ}C$ afforded yellow microcrystals, which were dried under vacuum. Yield: 105 mg, 51%; elemental analysis calcd (%) for $C_{47}H_{38}FeO_4P_2PtSi \cdot 0.5\,CH_2Cl_2$ (1050.75): C 54.32, H 3.74%; found C 54.50, H 3.62; ^{1}H NMR (300 MHz, $CDCl_3$): $\delta = 6.63-7.71$ (m, 35H; phenyl), 0.18 (s, ^3J(Pt,H) = 35 Hz, 3H; SiMe); ^{13}C{^{1}H} NMR (50.32 MHz, $CDCl_3$): $\delta = 210.9$ (d, ^2J(P,C) = 13 Hz, ^2J(Pt,C) = 46 Hz, Fe-CO), 143.4–126.5 (m, phenyl), 5.2 (br s, ^2J(Pt,C) = 75 Hz, SiMe); ^{29}Si-INEPT (HSi-HMQC) ($CDCl_3$): $\delta = -1.48$ (dd, ^2J(Pt,Si) = 10.9, 2.2 Hz, ^1J(Pt,Si) = 1509 Hz). Decomposition of this complex in solution affords inter alia $Ph_2MeSi-SiMePh_2$, characterized by its ^{29}Si-INEPT resonance at $\delta = -21.40$; this is particularly interesting since no siloxane was found.

[(OC)$_4$Fe(μ-PHCy)Pt{Si(OMe)$_3$}(CO)(PPh$_3$)] (10): A solution of **7e** (328 mg, 0.3 mmol) in CH_2Cl_2 (15 mL) was purged by a gentle stream of CO for 8 h and then stirred under a CO atmosphere overnight. The slow conversion from the initially formed intermediate **8e** to **10** was monitored by IR and ^{31}P{^{1}H} NMR spectroscopy. After evaporation of the solvent, the residue was extracted with Et_2O (10 mL); concentration of the solution and addition of hexane led to precipitation of crude orange **10**. Owing to the formation of small amounts of O=PPh$_3$ (ca. 15%, ^{31}P NMR: $\delta = 28.8$), which was formed during the CO-purge and could not be separated despite several attempts, no satisfactory elemental analyses could be obtained. ^{13}C{^{1}H} NMR (75.48 MHz, $CDCl_3$): $\delta = 210.2$ (d, ^2J(P,C) = 13 Hz, FeCO), 134.5–127.4 (m, phenyl), 49.4 (s, ^3J(Pt,C) = 19 Hz, SiOMe), 38.7–22.9 (m, C_6H_{11}); ^{29}Si-INEPT ($CDCl_3$): $\delta = -24.9$ (d, ^2J(Pt,Si) = 15 Hz, ^1J(Pt,Si) = 2523 Hz).

[(OC)$_3${(MeO)$_3$Si}Fe(μ-PPh$_2$)Pt(PPh$_3$)(CN*t*Bu)] (12a): *tert*-Butyl isonitrile (10 mg, 0.1 mmol) was added to a solution of **7a** (117 mg, 0.1 mmol) in CH_2Cl_2 (5 mL). After the mixture was stirred for 15 min, the bright yellow solution was concentrated under reduced pressure to about 1 mL, and the product precipitated upon subsequent addition of hexane (5 mL). The yellow product was filtered and dried in vacuo. Yield: 96 mg, 97%; elemental analysis calcd (%) for $C_{41}H_{43}FeNO_6P_2PtSi$ (986.13): C 49.91, H 4.39, N 1.42; found C 49.52, H 4.17, N 1.37; ^{1}H NMR: $\delta = 1.26$ (s, 9H; *t*Bu), 3.72 (s, 9H; SiOMe), 7.07–7.35 (m, 25H; phenyl).

[(OC)$_3${(MeO)$_3$Si}Fe(μ-PHCy)Pt(PPh$_3$)(CN*t*Bu)] (12b): *tert*-Butyl isonitrile (10 mg, 0.1 mmol) was added to a solution of **7e** (110 mg, 0.1 mmol) in CH_2Cl_2 (5 mL). After the solution was stirred for 15 min, all volatiles were removed under vacuum, and the solid residue triturated with hexane (5 mL) to remove PPh_3. The yellow product was then dried under vacuum. Yield: 87 mg, 95%; elemental analysis calcd (%) for $C_{35}H_{45}FeNO_6P_2PtSi$ (916.7): C 45.86, H 4.95, N 1.53; found C 45.65, H 4.92, N 1.50; ^{1}H NMR: $\delta = 7.25-7.75$ (m, 15H; phenyl), 5.01 (dd, ^1J(P,H) = 355 Hz, ^3J(P,H) = 4.1 Hz, ^2J(Pt,H) = 67.2 Hz, 1H; PH], 3.47 (s, 9H; SiOMe), 1.51–0.60 (m, 11H; C_6H_{11}), 1.30 (s, 9H; *t*Bu).

[(OC)$_3$(Ph$_2$MeSi)Fe(μ-PPh$_2$)Pt(PPh$_3$)(CN*t*Bu)] (12c): *tert*-Butyl isonitrile (10 mg, 0.1 mmol) was added to a solution of **7c** (117 mg, 0.1 mmol) in CH_2Cl_2 (5 mL). After the solution was stirred for 15 min, all volatiles were removed under vacuum, and the solid residue triturated with hexane (5 mL) to remove PPh_3. The yellow product was then dried under vacuum. Yield: 96 mg, 83%; elemental analysis calcd (%) for $C_{51}H_{47}FeNO_3P_2PtSi$ (1062.9): C 57.63, H 4.46, N 1.32; found C 57.53, H 4.22, N 1.24; ^{1}H NMR: $\delta = 7.07-7.35$ (m, 35H; phenyl), 1.20 (s, 3H; SiMe), 1.09 (s, 9H; *t*Bu).

[(OC)$_3${(MeO)$_3$Si}Fe(μ-PHCy)Pt(PPh$_3$)(CNxylyl)] (12d): Xylyl isonitrile (14 mg, 0.1 mmol) was added to a solution of **7e** (110 mg, 0.1 mmol) in CH_2Cl_2 (5 mL). After the solution was stirred for 15 min, the bright yellow solution was concentrated under reduced pressure to about 1 mL, and the product precipitated upon subsequent addition of hexane (5 mL). The yellow product was filtered and dried under vacuum. Yield: 87 mg, 90%; elemental analysis calcd (%) for $C_{39}H_{45}FeNO_6P_2PtSi$ (964.7): C 48.56, H 4.70, N 1.45; found C 48.92, H 4.91, N 1.38; ^{1}H NMR: $\delta = 7.05-7.71$ (m, 18H; phenyl), 5.05 (dd, ^1J(P,H) = 357 Hz, ^3J(P,H) = 4 Hz, ^2J(Pt,H) = 61 Hz, 1H; PH), 3.49 (s, 9H; SiOMe), 2.14 (s, 6H; xylyl-Me), 1.52–0.56 (m, 11H; Cy).

[(OC)$_3$(PhMe$_2$Si)Fe(μ-PPh$_2$)Pt(PPh$_3$)(CNxylyl)] (12e): Xylyl isonitrile (131 mg, 1.0 mmol) was added to a solution of **7b** (1180 mg, 1.0 mmol) in CH_2Cl_2 (50 mL). After the solution was stirred for 15 min, the bright yellow solution was concentrated under reduced pressure to about 6 mL, and the product was precipitated by addition of Et_2O (20 mL). The yellow product was filtered and dried under vacuum. Yield: 900 mg, 86%; elemental analysis calcd (%) for $C_{50}H_{45}FeNO_3P_2PtSi$ (1048.88): C 57.26, H 4.32, N 1.33; found C 57.18, H 4.65, N 1.40; ^{1}H NMR (200 MHz, C_6D_6): $\delta = 8.34-6.91$ (m, 33H; phenyl), 2.03 (s, 6H; xylyl-Me), 0.82 (s, 6H; SiMe).

[(OC)$_3$(Ph$_3$Si)Fe(μ-PPh$_2$)Pt(PPh$_3$)(CNxylyl)] (12f): Xylyl isonitrile (132 mg, 1.0 mmol) was added to a solution of **7d** (1304 mg, 1.0 mmol) in CH_2Cl_2 (50 mL). After 15 min the bright yellow solution was concentrated under reduced pressure to about 6 mL, and the yellow product was precipitated by addition of Et_2O (20 mL), filtered, and dried under vacuum. Yield: 1080 mg, 92%; elemental analysis calcd (%) for $C_{60}H_{49}FeNO_3P_2PtSi$ (1173.03): C 61.44, H 4.21, N 1.19; found C 60.98, H 4.22, N 0.96; ^{1}H NMR (200 MHz, CD_2Cl_2): $\delta = 8.44-6.61$ (m, 43H; phenyl), 1.86 (s, 6H; xylyl-Me).

X-ray structure analyses: A summary of crystal data, data collection, and structure analysis for compounds **2b**, **2c**, **3c**, **6**, and **12f** are given in Table 7. Data for **2b** and **2c** were collected on a Nonius CAD4-F diffractometer with $Mo_{K\alpha}$ graphite monochromated radiation ($\lambda = 71.069$ pm). The structures were solved by using direct methods and refined against $|F|$. Hydrogen atoms were introduced as fixed contributors. Absorption corrections derived from psi scans of seven reflections. For all computations the Nonius OpenMoleN package[40] was used. For both structures, all non-hydrogen atoms were refined anisotropically. The hydrogen atoms were calculated and fixed in idealized positions ($d_{C-H} = 95$ pm, $U_H = 1.3\,U_{equiv}$ for the carbon to which it was attached).

For the structures of **3c**, **6**, and **12f**, all measurements were done on an Enraf-Nonius four-circle CAD4 diffractometer with $Mo_{K\alpha}$ radiation ($\lambda = 71.069$ pm). The cell dimensions were determined by refinement of 25 high-angle reflections from different areas of the reciprocal space. Data were collected by the $\omega/2\theta$ scan method and corrected for Lorentz, polarization, and absorption effects (empirical absorption correction). The structures were solved by the Patterson method or direct methods, and refined by full-matrix least-squares. Hydrogen atoms were included in calculated positions. The *tert*-butyl groups of **3c** and **6** were disordered; several partially occupied positions were located which were isotropically refined.

Crystallographic data (excluding structure factors) for the structures reported in this paper have been deposited with the Cambridge Crystallographic Data Centre as supplementary publication no. CCDC-147167, CCDC-147168, CCDC-148246, CCDC-148247, CCDC-148248. Copies of the data can be obtained free of charge on application to CCDC, 12 Union Road, Cambridge CB2 1EZ, UK (fax: (+44) 1223-336-033; e-mail: deposit@ccdc.cam.ac.uk).

Acknowledgement

We are grateful to the Centre National de la Recherche Scientifique (associate research position to M.K.), the Ministère de l'Education Nationale, de l'Enseignement Supérieur et de la Recherche, the Commission of the European Communities (PhD grant to T.S., contract 913014) and the PROCOPE programme (stay of G.R. in Strasbourg) for financial support. We are very grateful to Prof. J. Fischer, Dr. A. DeCian and Dr. N. Kyritsakas (Strasbourg) for the X-ray diffraction study on **2b** and **2c**, and to Dr. J. Pfeiffer (Vienna, Austria) for recording the ^{29}Si-INEPT NMR spectrum of **9c**.

  0947-6539/00/0623-4276 $ 17.50+.50/0 *Chem. Eur. J.* **2000**, *6*, No. 23

Table 7. Summary of crystal data, data collection, and structure analysis.

	2b	**2c**	**3c**	**6**	**12f**
formula	$C_{20}H_{31}FeO_8PPtSi$	$C_{35}H_{25}FeO_5PPtSi \cdot 0.5\,C_6H_{12}$	$C_{43}H_{43}FeN_2O_3PPtSi$	$C_{33}H_{46}FeN_3O_6PPtSi$	$C_{60}H_{49}FeNO_3P_2PtSi$
M_w	709.46	877.66	945.83	890.75	1173.03
crystal size [mm]	$0.30 \times 0.30 \times 0.20$	$0.40 \times 0.40 \times 0.10$	$0.20 \times 0.20 \times 0.10$	$0.30 \times 0.50 \times 0.20$	$0.10 \times 0.20 \times 0.15$
crystal system	triclinic	monoclinic	monoclinic	monoclinic	monoclinic
space group	$P\bar{1}$	$C2/c$	$P2_1/c$	$C2/c$	$P2_1/n$
a [pm]	1054.2(3)	3574(1)	1701.8(6)	3800.4(13)	1202.7(5)
b [pm]	1085.9(3)	982.7(2)	1064.2(3)	1117.2(3)	1817.9(4)
c [pm]	1224.2(3)	2007.6(6)	2354.9(3)	2042.1(5)	2382.0(9)
α [°]	100.15(2)	90	90	90	90
β [°]	103.56(2)	93.69(2)	94.07(4)	112.13(4)	98.01(3)
γ [°]	94.98(2)	90	90	90	90
Z	2	4	4	8	4
ρ_{calcd} [g cm^{-3}]	1.773	1.657	1.477	1.473	1.510
T [K]	293	293	298	273	293
$V \times 10^6$ [pm^3]	1328	7037	4254.2	8031.4	5175
$\mu(Mo_{K\alpha})$ [cm^{-1}]	59.998	45.433	37.613	39.852	31.472
2θ range [°]	5–50	5–61	3–46	3–41	3-44
reflections collected	4681	9831	6520	8570	6947
data used [$I > 3\sigma(I)$]	3940	5515	6278	3454	6199
R_1[a]	0.024	0.034	0.047	0.040	0.038
wR_2[b]	0.037	0.047	0.058	0.048	0.042
residual electron density [e A^{-3}]	0.090	1.159	1.054	1.359	1.672
weighting scheme	$4F_o^2/(\sigma^2(F_o^2) + 0.0036F_o^4)$	$4F_o^2/(\sigma^2(F_o^2) + 0.0036F_o^4)$	$w = 1/\sigma(F)^2$	$w = 1/\sigma(F)^2$	$w = 1/\sigma(F)^2$

[a] $R_1 = \Sigma|F_o - F_c|/\Sigma|F_o|$. [b] $wR_2 = [\Sigma w(|F_o| - |F_c|)^2/\Sigma w(F_o)^2]^{1/2}$.

[1] a) B. J. Aylett, *Adv. Inorg. Chem. Radiochem.* **1982**, *25*, 1–133; b) T. D. Tilley in *Transition-Metal Silyl Derivatives* (Eds.: S. Patai, Z. Rappoport), Wiley, New York, **1991**, pp. 245–307; c) *Organosilicon Chemistry III, from Molecules to Materials* (Eds.: N. Auner, J. Weis), VCH, Weinheim, **1997**; d) *Organosilicon Chemistry II, from Molecules to Materials* (Eds.: N. Auner, J. Weis), VCH, Weinheim, **1996**; e) *Organosilicon Chemistry I, from Molecules to Materials* (Eds.: N. Auner, J. Weis), VCH, Weinheim, **1994**; f) U. Schubert, *Monatsh. Chem.* **1999**, *130*, 3–241; g) J. A. Gladysz, *Acc. Chem. Res.* **1984**, *17*, 326–332; h) H. Yamashita, M. Tanaka, *Bull. Chem. Soc. Jpn*. **1995**, *68*, 403–419.

[2] P. Braunstein, M. Knorr, *J. Organomet. Chem.* **1995**, *500*, 21–38.

[3] a) M. D. Curtis, P. S. Epstein, *Adv. Organomet. Chem.* **1981**, *19*, 213–255; b) H. Rabaâ, J.-Y. Saillard, U. Schubert, *J. Organomet. Chem.* **1987**, *330*, 397–413; c) D. Lichtenberger, A. Rai-Chaudhuri, *J. Am. Chem. Soc.* **1991**, *113*, 2923–2930; d) S. Sakaki, M. Ieki, *J. Am. Chem. Soc.* **1993**, *115*, 2373–2381; e) U. Schubert, *Angew. Chem.* **1994**, *106*, 435–437; *Angew. Chem. Int. Ed. Engl.* **1994**, *33*, 419–421; f) P. Hofmann in *Organosilicon Chemistry I, from Molecules to Materials* (Eds.: N. Auner, J. Weis), VCH, Weinheim, **1994**, pp. 231–250; g) J. B. Baruah, K. Osakada, T. Yamamoto, *Organometallics* **1996**, *15*, 456–459; h) H. K. Sharma, K. H. Pannell, *Chem. Rev.* **1995**, *95*, 1351–1374; i) J. Y. Corey, J. Braddock-Wilking, *Chem. Rev.* **1999**, *99*, 175–292, and references cited therein; j) N. K. Skvortsov, *Russ. J. General Chem.* **1993**, *65*, 661–687; k) W. Huang, C. E. Zybill, L. Luo, W. Hieringer, H. H. Huang, *Organometallics* **1998**, *17*, 5825–5829; l) C. E. Zybill, W. Huang, *Inorg. Chim. Acta* **1999**, *291*, 380–387; m) G. Kickelbick, U. Schubert, *Monatsh. Chem.* **1998**, *129*, 329–338.

[4] T. S. Piper, D. Lemal, G. Wilkinson, *Naturwiss.* **1956**, *43*, 129–129.

[5] P. Braunstein, M. Knorr, C. Stern, *Coord. Chem. Rev.* **1998**, *178–180*, 903–965.

[6] P. Braunstein, M. Knorr, T. Stährfeldt, *J. Chem. Soc. Chem. Commun.* **1994**, 1913–1914.

[7] P. Braunstein, M. Knorr, J. Cossy, P. Vogel, C. Strohmann, *New J. Chem.* **1999**, *23*, 1215–1222.

[8] a) P. Braunstein, X. Morise, J. Blin, *J. Chem. Soc. Chem. Commun.* **1995**, 1455–1456; b) P. Braunstein, X. Morise, *Organometallics* **1998**, *17*, 540–550; c) P. Braunstein, J. Durand, X. Morise, A. Tiripicchio, F. Ugozzoli, *Organometallics* **2000**, *19*, 444–450.

[9] P. Braunstein, X. Morise, *Chem. Rev.* **2000**, *100*, in press.

[10] a) M. Knorr, P. Braunstein, A. DeCian, J. Fischer, *Organometallics* **1995**, *14*, 1302–1309; b) M. Knorr, P. Braunstein, A. Tiripicchio, F. Ugozzoli, *Organometallics* **1995**, *14*, 4910–4919; c) P. Braunstein, J. Durand, G. Kickelbick, M. Knorr, X. Morise, R. Pugin, A. Tiripicchio, F. Ugozzoli, *J. Chem. Soc. Dalton Trans.* **1999**, 4175–4186; d) A. Sisak, A. Sironi, M. Moret, C. Zucchi, F. Ghelfi, G. Pályi, *J. Chem. Soc. Chem. Commun.* **1991**, 176–178.

[11] P. Braunstein, M. Knorr, B. Hirle, G. Reinhard, U. Schubert, *Angew. Chem.* **1992**, *104*, 1641–1643; *Angew. Chem. Int. Ed. Engl.* **1992**, *31*, 1583–1585.

[12] J. L. Speier, *Adv. Organomet. Chem*. **1979**, *17*, 407–447.

[13] P. Braunstein, M. Knorr, T. Stährfeldt, A. DeCian, J. Fischer, *J. Organomet. Chem.* **1993**, *459*, C1-C5.

[14] T. Blum, P. Braunstein, A. Tiripicchio, M. Tiripicchio-Camellini, *Organometallics* **1989**, *8*, 2497–2504.

[15] a) J. Powell, M. R. Gregg, J. F. Sawyer, *J. Chem. Soc. Chem. Commun.* **1987**, 1029–1031; b) J. Powell, M. R. Gregg, J. F. Sawyer, *J. Chem. Soc. Chem. Commun.* **1984**, 1149–1150; c) S. Rosenberg, W. S. Mahoney, J. M. Hayes, G. L. Geoffroy, A. L. Rheingold, *Organometallics* **1986**, *5*, 1065–1071; d) B. C. Benson, R. Jackson, K. K. Joshi, D. T. Thompson, *J. Chem. Soc. Chem. Commun.* **1968**, 1506–1507.

[16] a) J. Schwald, P. Peringer, *J. Organomet. Chem.* **1987**, *323*, C51–C53; b) H. C. Böttcher, M. Graf, K. Merzweiler, *J. Organomet. Chem*. **1996**, *525*, 191–197; c) E. Keller, H. Vahrenkamp, *Chem. Ber.* **1979**, *112*, 2347–2368.

[17] P. Braunstein, M. Knorr, B. E. Villarroya, A. DeCian, J. Fischer, *Organometallics* **1991**, *10*, 3714–3722.

[18] M. Knorr, P. Braunstein, A. Tiripicchio, F. Ugozzoli, *J. Organomet. Chem.* **1996**, *526*, 105–116.

[19] P. J. Hay, *Theoretical Studies of Oxidative Addition and Reductive Elimination of Hydrogen and Alkanes* (Ed.: A. Dedieu), VCH, Weinheim, **1992**, pp. 127–147.

[20] P. Braunstein, T. Faure, M. Knorr, T. Stährfeldt, A. DeCian, J. Fischer, *Gazz. Chim. Ital.* **1995**, *125*, 35–50.

[21] M. Green, A. Laguna, J. L. Spencer, F. G. A. Stone, *J. Chem. Soc. Dalton Trans.* **1977**, 1010–1016.

[22] a) M. Knorr, T. Stährfeldt, P. Braunstein, G. Reinhard, P. Hauenstein, B. Mayer, U. Schubert, S. Khan, H. D. Kaesz, *Chem. Ber.* **1994**, *127*, 295–304; b) G. Reinhard, M. Knorr, P. Braunstein, U. Schubert, S. Khan, C. E. Strouse, H. D. Kaesz, A. Zinn, *Chem. Ber.* **1993**, *126*, 17–21; c) P. Braunstein, T. Stährfeldt, J. Fischer, *C. R. Acad. Sci. Ser. 2 c* **1999**, 273–282.

[23] P. Braunstein, M. Knorr, H. Piana, U. Schubert, *Organometallics* **1991**, *10*, 828–831.

[24] a) E. A. V. Ebsworth, V. M. Marganian, F. J. S. Reed, R. O. Gould, *J. Chem. Soc. Dalton Trans.* **1978**, 1167 – 1170; b) M. Knorr, S. Kneifel, C. Strohmann in *Organosilicon Chemistry III, from Molecules to Materials* (Eds.: N. Auner, J. Weis), VCH, Weinheim, **1997**, pp. 211 – 216; c) L. S. Chang, M. P. Johnson, M. J. Fink, *Organometallics* **1989**, *8*, 1369 – 1371.
[25] H. Inoue, T. Nakagome, T. Kuroiwa, T. Shirai, E. Fluck, *Z. Naturforsch. Teil B* **1987**, *42*, 573 – 578.
[26] J. Chatt, C. Eaborn, S. D. Ibekwe, P. N. Kapoor, *J. Chem. Soc. A* **1970**, 1343 – 1351.
[27] M. Green, J. A. K. Howard, M. Murray, J. L. Spencer, F. G. A. Stone, *J. Chem. Soc. Dalton Trans.* **1977**, 1509 – 1514.
[28] a) W. Jetz, W. A. G. Graham, *J. Organomet. Chem.* **1974**, *69*, 383 – 387. b) M. A. Guerra, R. J. Lagow, *J. Chem. Soc. Chem. Commun.* **1990**, 65 – 66.
[29] M. T. Reetz, *Adv. Organomet. Chem*. **1977**, *16*, 33.
[30] J. C. Calabrese, L. F. Dahl, *J. Am. Chem. Soc.* **1971**, *93*, 6042 – 6047.
[31] A. Heine, D. Stalke, *Angew. Chem.* **1993**, *105*, 90 – 92; *Angew. Chem. Int. Ed. Engl*. **1993**, *32*, 121 – 122.
[32] K. Osakada, T.-A. Koizumi, T. Yamamoto, *Angew. Chem.* **1998**, *110*, 364 – 366; *Angew. Chem. Int. Ed.* **1998**, *37*, 349 – 351.
[33] a) M. Akita, T. Oku, R. Hua, Y. Moro-Oka, *J. Chem. Soc. Chem. Commun.* **1993**, 1670 – 1672; b) M. Akita, R. Hua, T. Oku, M. Tanaka, Y. Moro-Oka, *Organometallics* **1996**, *15*, 4162 – 4177.
[34] a) W. Lin, S. R. Wilson, G. S. Girolami, *J. Am. Chem. Soc.* **1993**, *115*, 3022 – 3023; b) W. Lin, S. R. Wilson, G. S. Girolami, *Organometallics* **1994**, *13*, 2309 – 2319; c) Q. D. Shelby, W. Lin, G. S. Girolami, *Organometallics* **1999**, *18*, 1904 – 1910.
[35] E. M. López, D. Miguel, J. Pérez, V. Riera, C. Bois, Y. Jeannin, *Organometallics* **1999**, *18*, 490 – 494.
[36] C. A. Tolman, *Chem. Rev.* **1977**, *77*, 313 – 348.
[37] E. L. Eliel, N. L. Allinger, S. J. Angyal, G. A. Morrisson, *Conformational Analysis*, Interscience, New York, **1965**, p. 191.
[38] J. Powell, E. Fuchs, M. R. Gregg, J. Phillips, M. V. R. Stainer, *Organometallics* **1990**, *9*, 387 – 393, and references therein.
[39] P. Braunstein, T. Faure, M. Knorr, *Organometallics* **1999**, *18*, 1791 – 1794.
[40] OpenMoleN, *Interactive Structure Solution*, Nonius, Delft (The Netherlands), **1997**.

Received: March 13, 2000 [F2358]

  0947-6539/00/0623-4278 $ 17.50+.50/0